A THERMODYNAMIC APPROACH FOR COMPACTION OF ASPHALTIC COMPOSITES

A Thesis

by

SARADHI KONERU

Submitted to the Office of Graduate Studies of
Texas A&M University
in partial fulfillment of the requirements for the degree of

MASTER OF SCIENCE

December 2006

Major Subject: Mechanical Engineering

A THERMODYNAMIC APPROACH FOR COMPACTION OF ASPHALTIC COMPOSITES

A Thesis

by

SARADHI KONERU

Submitted to the Office of Graduate Studies of
Texas A&M University
in partial fulfillment of the requirements for the degree of

MASTER OF SCIENCE

Approved by:

Co-Chairs of Committee,	Dr. K. R. Rajagopal
	Dr. Eyad Masad
Committee Members,	Dr. N. K. Anand
Head of Department,	Dr. Dennis O'Neal

December 2006

Major Subject: Mechanical Engineering

ABSTRACT

A Thermodynamic Approach for Compaction

of Asphaltic Composites. (December 2006)

Saradhi Koneru, B.E, Osmania University, India

Co–Chairs of Advisory Committee: Dr. K. R. Rajagopal
Dr. Eyad Masad

This thesis studies the mechanics which can be associated with asphalt concrete compaction and develops continuum models in a general thermo-mechanical setting which can be used in future work to corroborate experimental compaction experiment results. Modeling asphalt concrete compaction, and also the ability to thereby predict response of mixes, is of great importance to the pavement industry.

Asphalt concrete exhibits nonlinear response even at small strains and the response of asphalt concrete to different types of loading is quite different. The properties of asphalt concrete are highly influenced by the type and amount of the aggregates and the asphalt used. The internal structure of asphalt concrete continues to evolve during the loading process. This is due to the influence of different kinds of activities at the micro-structure level and to the interactions with the environment. The properties of asphalt concrete depend on its internal structure. Hence, we need to take into account the evolution of the internal structure in modeling the response of asphalt concrete.

A theoretical model has been developed using the notion of multiple natural configurations to study a variety of non-linear dissipative responses of real materials. By specifying the forms for the stored energy and the rate of dissipation function of

the material, a specific model was developed using this framework to model asphalt compaction. A compressible model is developed by choosing appropriate forms of stored energy and rate of dissipation function. Finally, a parametric study of the model is presented for a simple compression deformation. It is anticipated that the present work will aid in the development of better constitutive equations which in turn will accurately model asphalt compaction both in laboratory and in field. Distinct numerical approaches have been used to demonstrate the applicability of the theoretical framework to model material response of asphalt.

To Mother, Father and my loving Sisters

ACKNOWLEDGMENTS

I would like to express my sincere gratitude to Prof. K.R. Rajagopal for giving me this excellent opportunity to work with him. During my studies in graduate school, I have and continue to learn a great deal from his vast knowledge in mechanics, mathematics and general aspects of life. His demand for the pursuit of knowledge has always inspired and challenged me to put forth my best effort in my studies and research activities. Prof. Rajagopal's lectures on continuum mechanics, elasticity and nonlinear mechanics were captivating and his special style of teaching always keeps me enthusiastic about the subject of mechanics. His discourses on various aspects of mechanics both during group meetings and during our personal interactions have helped me think critically. The freedom that he gave me in pursuing my ideas during the course of my research work has helped me prepare mentally to work as an independent researcher.

I thank Prof. Masad whose class on bituminous materials guided my initial foray into asphalt mechanics and helped me develop an understanding of the subject. I have always found him very enthusiatic in our discussions as he explains the many things I haven't the complete grasp of. I gratefully appreciate the time he has always given me and the help and support he readily extends whenever I need it. I also thank him for the patience he has shown me during the course of this work.

I would also like to take this opportunity to thank Prof. N. K. Anand for serving on my committee and would also like to thank Dr. J. MuraliKrishnan and Dr. Krishna Kannan for their support and valuable advice and for helping me out when I lacked understanding of some key issues. My numerous discussions on various issues related to my research work and mechanics in general with Dr. Krishna Kannan and Dr. Parag Ravindran have helped me think clearly and analyze issues with a broader

perspective.

I thank Dr. Luoyi Tao for imparting some of his vast knowledge and wisdom during our talks. I admire his simplicity and his incisive intelligence. He will always inspire me. Let me also take this opportunity to thank my seniors and colleagues, Dr. Anand Mohan, Waqar Malik, Song Min Jae, Craig Bridges and Kiran Narayanan, for the many discussions and talks we frequently have. Such discussions have helped me improve the scope of my knowledge and also serve as a reminder what I still need to learn. I would also like to gratefully acknowledge the support and friendship of my close friends who have certainly made my stay here utterly enjoyable.

I am also grateful for all the love, support and encouragement that I received from my family and friends. I am deeply indebted to my parents for imbibing me with the desire to and the belief needed to always put my best efforts into all my endeavors. Also, some of the results of the current work were obtained using the Supercomputing facility at Texas A&M University and I wish to acknowledge the facilities provided by them and their ready support.

TABLE OF CONTENTS

CHAPTER Page

LIST OF TABLES

LIST OF FIGURES

FIGURE Page

FIGURE Page

CHAPTER I

INTRODUCTION

This study primarily focusses on examining the compaction behavior of Hot Mix Asphalt(HMA). Reviewing some of the literature [4,6,13] which provide an account of the fascinating history, uses and importance of asphalt and its derivative material mixtures, we come to realize that asphalt has been used for varied applications since ancient times. The unique properties of asphalt, such as its adhesion/bonding strength, waterproofing and even its use as a fuel in lamps meant that it has always served an important role in human history.

Asphalt pavements account for approximately 2.3 million miles of American hard surfaced roadways. The importance of roads can be understood from the fact that Americans traveled 2.7 trillion vehicle miles in the year 2000 [4,6] and, about 54 percent of total freight transport by weight and 83 percent by value in 1998 occurred over the highways [21]. The substantial size of asphalt-based industry can be gauged from the fact that Europe and USA produced 800 million tons of HMA in the year 2003 [4].

HMA is a composite material that is made up of asphalt as a binder mixed with filler/fines(together with the asphalt called the mastic) and aggregates (processed and graded rocks). Aggregates finer than .075 mm added to the mixture are classified as fillers or fines. The fillers and the aggregates play two distinct roles in determining the methanical properties exhibited by the material. In general, the addition of fillers stiffens the mix, affects aging characteristics, and resistance to distresses such as fatigue cracking and permanent deformation (rutting). The final mixture laid on the

---

The journal model is *IEEE Transactions on Automatic Control*.

field and also the specimens made in the laboratory for studying HMA necessarily (due to the different sizes and shapes of aggregates used) include air voids. The presence of such air voids is very much determined by the process of 'Compaction', wherein the loose mixture is consolidated into a denser material by application of external loads. We shall call such loading actions, in a generic sense, the 'Compaction Effort'.

The mix compaction is an important process that influences pavement performance. Poorly compacted mixtures with high percent air voids are susceptible to moisture infiltration, oxidation and cracking. On the other hand, mixtures compacted to have very low air voids are susceptible to asphalt bleeding in hot weather environments.

Very little research has been directed in the past towards modeling HMA compaction and the material properties that influence the mix compactibility. A mechanistic model for compaction can be very useful for engineers to predict mix compatibility prior to expensive and time consuming trials of building test sections before the pavement construction.

Our chief endeavour in regard to Asphalt mechanics is to be able to develop theoretically sound mathematical models which adequately describe the observed compaction characteristics in HMA. As such we seek to solve the specific a initial-boundary value problem that is representative of the physical situation arising in a SUPERPAVE gyratory compactor.

A. Goals and Focus of Current Work

In this work, the aim is to develop a constitutive theory within the context of continuum mechanics, to study compaction of HMA. The goal of such continuum theories is to describe the macroscopic behavior of a material without explicitly going into

the complex details at the microscopic level, while at the same time taking a consideration of the microstructure , albeit in a homogenized sense. As such we shall pursue the aim of developing a thermodynamic continuum model for the description of Asphalt Concrection process. A parametric study is thereafter taken up to help establish the theoretical basis for the ability to perform analytical studies on asphalt concrete compaction. This will serve the author in his pursuits in further studies and investigations into modeling compaction.

Using the theoretical framework put in place by Rajagopal [31] and co-workers to study the response of dissipative bodies, a large deformation model for asphalt mixtures is developed and corroborated with using the experimental results for compaction. The constitutive model is within a thermodynamic setting and it exploits the fact that the configuration that the body would attain on the removal of external stimuli, referred to as its "natural configuration", evolves, with the response of the body being non-dissipative (in general situations, non-entropy producing) from these evolving "natural configurations". The evolution of these natural configurations is determined by the assumed tendency of the body to undergo a process that maximizes the rate of dissipation.

B. Outline of the Thesis

Following this brief introduction in Chapter I; Chapter II includes the relevant information and literature pertaining to the current work on Compaction. Chapter III, contains a detailed documentation of the experimental procedure followed for obtaining data on the compaction of different mixture samples. In Chapter IV, the preliminaries that form the backbone of the current work is discussed. The kinematics, kinetics, balance laws in continuum mechanics, second law of thermodynamics

and the notion of frame invariance is discussed. An isothermal constitutive model for the compaction of HMA is developed. Chapter V deals with incorporating the constitutive model in a finite element software ABAQUS as a User Material (UMAT) to enable its use for solving more general problems and the methodology adopted to solve the specific problem of and the results are presented. In Chapter VI, discussion of results, a summary of the thesis and recommendations for future work is presented.

C. Notations Used

The notations used in this dissertation are similar to those used in standard continuum mechanics texts. Vectors and Tensors (second order and fourth order tensors) are represented with bold faced letters. As such we have,

a- A Vector,

T- A Second order tensor,

K- A Fourth order tensor.

The gradient and divergence operator with respect to initial reference configuration are denoted as:

$Grad\,\mathbf{a} = \frac{\partial \mathbf{a}}{\partial \mathbf{X}}, \quad [Grad\,\mathbf{a}]_{\mathbf{ij}} = \frac{\partial a_i}{\partial X_j},$

$Div\,\mathbf{T} = \frac{\partial \mathbf{T}}{\partial \mathbf{X}}, \quad [Div\,\mathbf{T}]_{\mathbf{i}} = \frac{\partial T_{ij}}{\partial X_j}.$

The gradient and divergence operator with respect to current configuration are denoted as:

$grad\,\mathbf{a} = \frac{\partial \mathbf{a}}{\partial \mathbf{X}}, \quad [grad\,\mathbf{a}]_{\mathbf{ij}} = \frac{\partial a_i}{\partial X_j},$

$div\,\mathbf{T} = \frac{\partial \mathbf{T}}{\partial \mathbf{X}}, \quad [div\,\mathbf{T}]_{\mathbf{i}} = \frac{\partial T_{ij}}{\partial X_j}.$

CHAPTER II

LITERATURE REVIEW

HMA is a mixture of asphalt and aggregates with sizes ranging from a maximum size that can be 25 mm to a fine filler of about 0.075 mm in size. Since HMA is made of granular materials which are bound together by a viscoelastic fluid, its behavior is a function of the loading and environmental conditions. Asphalts from different crude sources have completely different properties. The method of separation of asphalt from the crude and the processing method has an important influence on the mechanical response of asphalt. In addition to this, asphalt is extremely sensitive to temperature. The interaction between the aggregate particles is highly influenced by the size, shape, angularity and surface roughness of the constituent particles. Since the behavior of HMA depends on the non-linear interaction between the aggregate particles themselves and with asphalt, it is an extremely difficult material to model.

Evaluation of the performance of asphalt mixtures is done through laboratory testing. The laboratory HMA specimens should be fabricated in a manner that adequately simulates field pavements in order for laboratory testing to yield reliable mechanical properties. It is known that the HMA is a heterogenous material as it consists of aggregates, asphalt binder, and air voids. These three constituents in laboratory specimens should match with the ones in the field. The air void is a major factor that affects the performance of asphalt mixtures [24]. Only the average percent air voids is usually matched between laboratory specimens and asphalt pavements. However, quantifying the air void distribution by an average value is not sufficient to due to the heterogeneous nature of air void distribution through the specimen. Ignoring the heterogeneous nature of air void distribution could have critical impact on the design, testing, and development of performance models of asphalt mixtures

[11,24]. Testing specimens with nonuniform distributions of air voids causes high variation in stresses and strains within a specimen thus affecting testing repeatability and eventually misrepresenting the material response [11,24]. The laboratory compacted specimens should have a homogenous air void distribution for reliable estimation of the performance of asphalt mixtures in the field [11,20,24].

In order to obtain reliable mechanical properties from a laboratory performance test, it is necessary to ensure that laboratory specimens are fabricated to adequately represent field compaction. It is valuable to notice that differences in air void distributions between asphalt mixes can occur even at the same percent air voids. This could be due to the differences in compaction method, aggregate shape, aggregate size distribution, and target volumetric values. By differences in air void structure we mean the gradients in air void distributions (i.e, spatial changes air void percentages with depth), and the different air void size distributions. The differences in air void distributions are also evident when a comparison is drawn between different asphalt pavements [11,20,24]. Some asphalt pavements tend to have significantly higher percent air voids in the top one inch than the rest of the pavement [11,20,24]. Water tends to flow in such air voids percent portions in the pavement where traffic loading also is the highest. Coarser graded HMA mixtures, such as coarse matrix-high binder (CMHB) and SUPERPAVE coarser gradations, have a higher tendency to produce mixtures with permeable air voids than conventional dense-graded mixtures. Several studies have clearly shown that differences in the air void structure lead to significant differences in performance. Large voids promote faster damage growth under tensile loading leading to a reduction in fatigue life. Moisture damage is also found to be related to the air void structure. A uniform air void distribution throughout the sample reduces the localization of high strains in the mix, and improves performance. These findings emphasize a pressing need to understand the air void distributions

and its influence on performance. Such understating is necessary to design and construct asphalt pavement with optimum air void structure, and consequently, improved performance.

From various previous studies, it is concluded that a mixture that is properly designed and compacted should contain enough air voids to prevent rutting due to plastic flow but low enough air voids to prevent permeability of air and water. Since density of asphalt mixture varies throughout its life the voids must be low enough initially to prevent permeability of air and water and high enough after a few years of traffic to prevent plastic flow. Hence, the importance of proper and adequate compactive effort needs to be understood and duely recognised.

A. Compaction of Hot Mix Asphalt

Compaction is the process by which the volume of asphalt mixture is reduced. Compaction reduces the air voids in the HMA and increases the unit weight through the application of external forces. As a result of the compaction process the aggregate interlock and interparticle friction increases. Compaction has a significant influence on the HMA performance in the field, providing all desirable mix design characteristics. Inadequate compaction will lead to poor asphalt pavement performance. Adequate compaction decreases the rutting, increases fatigue life, decreases moisture damage and decreases low temperature cracking

B. Factors Affecting Compaction

There are some factors that affect HMA compaction. These factors include the properties of the materials in the mixture, environmental variables, conditions at the laydown site, and the method of compaction being used [11]. The field compaction

equipment and laboratory compaction equipment will be discussed in subsequent sections.

1. Properties of Constituent Materials

a. Aggregate Properties

In generalcompactive effort increases with the increase of the aggregate angularity, nominal maximum aggregate size, and hardness of aggregate used. Angular aggregate requires more densification effort due to its resistance to reorientation. The surface texture of aggregates affect the compactive effort whereas, smooth surface aggregates is easier to compact than the ones that have rough surface. The shape of the aggregate is also an important factor. For example, the rounded shape aggregates need less compactive effort than cubical or block-shaped aggregate.

b. Asphalt Binder

The ability to densify/compact the asphalt mixtures is affected by the grade and amount of asphalt binder [42]. A mix produced with high grade binder is usually stiff and need more compactive effort to obtain the desired density. The asphalt binder content also influences the compactive effort. A mix produce with too little amount of asphalt binder is stiff and usually needs more compactive effort than the mix with high asphalt binder. Also, we should take note of the temperature susceptibility of the asphalt binder that affects the workability and the time available for compaction [3,21,42].

C. Compaction Equipment

The density of asphalt layer is affected by the method of compaction being used. Different density levels can be obtained at the same number of passes when different compaction equipment is used. Let us now review a few of the field compaction and laboratory compaction equipment in the following sections.

1. Field Compaction Equipment

It was mentioned previously that compaction reduces air voids and increases the unit weight through the application of external forces. In the field, compaction is done in order to achieve the following objectives [1]:

- To obtain the desired density level and meet the specifications
- To provide the roadway with a smooth surface.

The compaction equipment can be divided into three general categories; static steel wheel rollers, pneumatic tire rollers, and vibratory steel wheel rollers.

a. Static Steel Wheel Rollers

A static steel wheel is a self-propelled compaction device. Static steel wheel rollers weight between 3 to 14 tons however its weight can be changed by adding ballast. The diameter of its drum varies from 1.0 to 1.5 m [16]. The effective contact pressure between the steel drum and the asphalt layer being compacted determines the actual compactive effort supplied by the roller [1,16]. Static steel rollers equipped with large drums have lower angles of contact than those provided with small drums and so have a lower horizontal component of force, that tends to push against the asphalt layer being compacted [1,16].

b. Pneumatic Tire Rollers

Pneumatic tire rollers are usually used for intermediate rolling behind the static steel wheel or vibratory steel wheel and in front of a static steel roller finish roller. Occasionally, pneumatic rollers used for initial or finish rolling. There are many factors influence the compactive effort applied by the pneumatic roller. These factors include the wheel load of the rollers, the tire pressure, the tire design, and the depth of penetration of the tire into the mix [1].

c. Vibratory Steel-Wheel Rollers

Vibratory steel- wheel rollers have a dynamic load component and their weight is lighter than the static steel wheel roller. The dynamic load of the roller is produced by attaching an eccentric weight to the rotating shaft in the center of the drum. The drum diameters are 1.02 to 1.52 m, and the drum widths between 1.47 and 2.13 m. The compactive effort supplied by the vibratory rollers is influenced by the static and dynamic load of the machine; however the dynamic load is the significant force in densification of the asphalt layer.

2. Laboratory Compaction Equipment

Many compaction devices have been used to compact HMA specimens in the laboratory with the aim of simulating the asphalt mixtures in the field. These compaction devises include for instance; Texas gyratory shear devices, California kneading compactor, Marshall impact compactor, mobile steel wheel simulator, Arizona vibratory-kneading compactor, and Superpave gyratory compactor.

The Superpave gyratory compactor, shown in Figure 1, is used to compact HMA specimens in the laboratory. There are some similarities between the SGC and other

Fig. 1. Servopac Gyratory Compactor.

gyratory compactors; however the SGC is a unique device. The parameters that control the compaction effort of the SGC are vertical pressure, angle of gyration, and number of gyrations. Differences in compaction parameters of the SGC produce HMA specimens with different internal structure which is represented by air void distribution, aggregate orientation and aggregate contacts.

D. Past Attempts at Modeling Compaction

Here, a brief review of some relevant efforts on modeling compaction is presented.

Most compaction modeling attempts have been aimed at quatifying and describing the internal structure, either throught image analyses[18,20] or through computer simulation of the structures[18,24]. Very few models have been proposed in the form of mathematical relations to predict behavior of asphalt mixes in the context of compaction. Also, some attempts are being made at using soil compaction modeling techniques to model HMA mixtures. Such efforts need to take a careful and guarded approach to using soil compaciton modeling techniques to model HMA compaction

as it will give rise to many problems simply due to the presence a highly nonlinear and complex material as asphalt.

There have been some attempts to mechanistically model the compaction process. Here, a brief review of some relevant efforts on mechanical modeling compaction is presented.

1. The Porous Elastic-Plastic Compaction Model

A porous elasto-plastic compaction model has been formulated based on Gursons porous material model by Guler et. al., which uses certain model constants to determine measured deflections of a gyratory compactor by means of nonlinear parameter estimation. An incremental constitutive relation for porous material was formulated for this purpose. The approach is primarily concerned with obtaining statistically significant parameters for this constitutive relation and obtaining a correlation with mixture variables, i.e., volumetric properties, particle size, that would enable an evaluation of the effects of mixture properties on the estimated model constants. This, thereby, provides mixture properties that give best correlations with the parameters. However, this approach doesnot provide a phenomenological model describing and ,in turn, derived form the physics of material behavior.

2. The Critical State Theory Approach

To analyze HMA its behavior during compaction was investigated in terms of elastic-plastic-viscous behavior. The results obtained at an increasing compaction level show that the behavior at the start of the compaction process is largely plastic and hardly elastic and viscous. When the material becomes compacted this turns over in largely elastic and just little viscous and plastic. The essence of such a model is that it couples a change in specific volume of the material to the stress state of that material.

The constitutive model for HMA was adopted from soil mechanics using the elastic-plastic principles, called the critical state theory. The critical state theory describes granular material behavior by means of a closed yield locus. Different shapes of yield loci are used for different granular materials. A yield locus gives a boundary between stress states that cause elastic (recoverable) deformations and plastic (irrecoverable) deformations. If a stress point falls inside a yield locus, the material behaves elastically, if the stress point falls on the yield locus, the material behaves plastically. However, we need to remember that a stress point can never fall outside a yield locus as the yield locus is a limitation of possible stress states. Preliminary simulations of the rolling process(representing rolling to achieve compaction) showed that during the process high isotropic stress situations occurred in the material. This implies that plastic deformations due to these compaction stress situations cannot be simulated. This makes the Mohr-Coulomb model inadequate for modeling compaction processes of HMA.

The above description for the application of the critical state theory to model the behavior of HMA compacted mixes gives a qualitative characterization of the material behavior. Through experimental methods the critical state parameters were obtained, thereby helping to determine the yield loci to obtain the material response characteristics.

To develop simulations of the compaction process a FEM approach was used. The approach taken to material modeling governs that the material behaves partly as a solid and partly as a liquid. A suitable material model should be available for use inside the FEM. A suitable approach for the problem was the ALE method; a mixed approach between Eulerian and Lagrangian methods. From the results of the numerical simulation it was evident the elastic part of the model did not correspond to the equivalent part of the critical state model, therefore a validation through a

comparison between the test section and simulations achieved could not been done using his modeling approach.

A recent work, by Murali Krishnan et.al.[24,25], which presents a constitutive model for asphalt mixes based on the mixture theory hypothesis, was used to obtain predictive data pertaining to certain mix characteristics. This model was proposed within the frame work of mixture theory in continuum mechanics and hence takes appropriate account of the physics of HMA mixtures. It utilizes the fundamental balances laws to obtain mathematical relations to describe the performance and characteristics of bituminuos mixes. However the appropriateness of such an approach to modeling compaction of HMA has yet to be considered due to the restrictive experimental techniques available to us to measure the mixture variables involved in the model.

CHAPTER III

COMPACTION EXPERIMENTS ON ASPHALT CONCRETE MIXES

A. Introduction

The response of the asphalt concrete specimens to constant loads are measured at different compaction inclinations angles for the experimental setup described henceforth. The method of preparation of the asphalt concrete samples and the experimental procedure are also presented here. The total height of the specimen as the gyrations of the compactor take place were measured and documented. The experiments were carried out for four different mix designs at three different mould inclinations and two loads in each case.

B. Sample Preparation

The preparation of test samples require utmost care and patience to ensure identical samples. Each step in the preparation process is crucial in determining the final response of the asphalt concrete specimens. For instance a reduction of aggregate fines of 3 % can produce a change in fatigue life of up to 300% (Harvey and Monismith, 1993). The American Society for Testing and Materials (ASTM) has laid down detailed guide lines and testing procedures in order to standardize the testing procedure and the methods of preparation. Dessouky followed the ASTM guidelines in the preparation of the test specimens. Broadly, the preparation of the sample can be classified into the following:

- Separation of aggregates into different aggregate size fractions
- Mix design

- Prepare batch mixes
- Preheat the batch mixes and asphalt
- Batch mixing of asphalt and aggregate
- Oven aging
- Compaction using a gyratory compactor
- Air void determination

1. Aggregate Separation

The aggregates used in the highway construction are largely obtained from local supplies of natural rock. The properties of the final test sample are largely determined by the overall size of the aggregates and the relative percentages of various sizes of aggregates in the sample. In order to ensure the same relative percentages of sizes of aggregates in the final sample, one needs to blend the aggregates keeping the relative percentage of aggregate sizes constant. Hence it is important that the aggregates are first separated into different sized particles which is done through sieving. Sieves typically used for sieve analysis are: 1 inch, 3/4 inch, 1/2 inch, 3/8 inch, No. 4, No. 8, No. 16, No. 30, No. 50, No. 100 and No. 200. A 3/8 inch sieve has openings equal to 3/8 inch. A No. 8 sieve has 8 openings per inch. A No.8 sieve size will be smaller than 1/8 inch, since the diameter of the wire should also be taken into consideration when calculating the sieve size. The sizes of successive sieves usually differ by a factor of 2.

The objective of a mix design is to determine the right combination of asphalt cement and aggregate that will give a stable and strong pavement structure. Mix design involves selecting the appropriate blend of aggregate sources to produce a proper

gradation of mineral aggregate, and selecting the type and amount of asphalt to be used as a binder for that gradation. Aggregate gradation is the distribution of particle sizes expressed as a percent of the total weight. The gradation of an aggregate is normally expressed as total percent passing various sieve sizes. Gradation of an aggregate can be graphically represented by a gradation curve for which the ordinate is the total percent by weight passing a given size on an arithmetic scale, while the abscissa is the particle size plotted to a logarithmic scale. The gradation of an aggregate is determined by a sieve analysis. Standard proecdures for a dry sieve analysis are given in ASTM C136. Gradation is one of the most important properties of the aggregate. It influences all the important properties of the asphalt concrete specimen including its strenght, durability, permeability, workability, moisture susceptibility etc. It might seem reasonable to assume that the best gradation is the one that gives the densest particle packing. This densest packing will provide increased stability through increased interparticle contacts and reduced air voids in the aggregate matrix. However a sufficient amount of air voids is required in the asphalt concrete to incorporate enough asphalt cement to ensure durability. Also some amount of air voids is necessary in the mixture to avoid bleeding and rutting of the pavements. Another unwanted effect of the dense packing is that the mixture will be more sensitive to slight changes in the asphalt content.

Most specifications for HMA (Hot Mix Asphalt) require well or dense graded aggregate gradations with the middle portion of the curves approximately parallel to the maximum density curves. ASTM D 3515 recommends some gradation limits to be used with asphalt mixtures. This is has been shown in table I.

The most common method of determining the proportions of aggregate to use to meet specification requirements is through trial and error. A trial blend is selected and calculations are made to determine the percent passing each sieve size for the blend.

This grading is then compared with the specification requirements. The process is repeated for the critical sieves until a satisfactory or optimum blend is obtained.

Table I. Types of Aggregates

Aggregates	Gradation	Size, in mm	% Fine Aggregate	Design AC %	Mix Label
Limestone	Coarse	19	0	4.4	C
			40	4.7	D
Gravel	Coarse	19	0	5.4	K
			40	4.8	L

Results of the seive analysis for the different mix designs used by Dessouky[x] is tabulated next.

2. Mix Design

Determination of Air Voids For determining the air voids, it is first necessary to calculate both the theoretical maximum specific gravity (Rice specific gravity) of the mix and also the bulk specific gravity of the compacted asphalt concrete specimen. The ratio of the weight in air of a unit volume of an uncompacted bituminous paving mixture (without air voids) at a stated temperature to the weight of an equal volume of a gas-free distilled water at a stated temperature is called the Rice Specific Gravity of the mixture. The test method for finding the theoretical maximum specific gravity of bituminous paving mixtures is described in AASHTO T209. The theoretical maximum specific gravity can be determined by the following equation:

$$G_{mm} = \frac{\text{A}}{\text{A - C}}$$

Table II. Gradations for the Four HMA Mix Designs

Sieve Size/ Total Mass/ Binder(%wt.)	Seive Size (mm)	Design HMA Mixtures			
		Mix designation and Weights of Aggregates (in gms)			
		Mix C	Mix D	Mix K	Mix L
1 - 3/4	25 - 19	360	410	270	315
3/4 - 1/2	19 - 12.5	756	864	500	581
1/2 - 3/8	12.5 - 9.5	626	536	405	450
3/8 - #4	9.5 - 4.75	1305	824	1238	1157
#4 - #8	4.75 - 2.36	410	194	752	374
#8 - #16	2.36 - 1.18	351	221	518	243
#16 - #30	1.18 - 0.6	243	441	347	441
#30 - #50	0.6 - 0.3	162	792	216	792
#50 - #100	0.3 - 0.15	81	140	131	95
#100 - #200	0.15 - 0.075	36	9	68	9
< #200	< 0.075	171	72	59	45
TOTAL		4500	4500	4504	4500
PG Grade		76-22(5.2%)	64-22(4.7%)	76-22(5.4%)	64-22(5.6%)

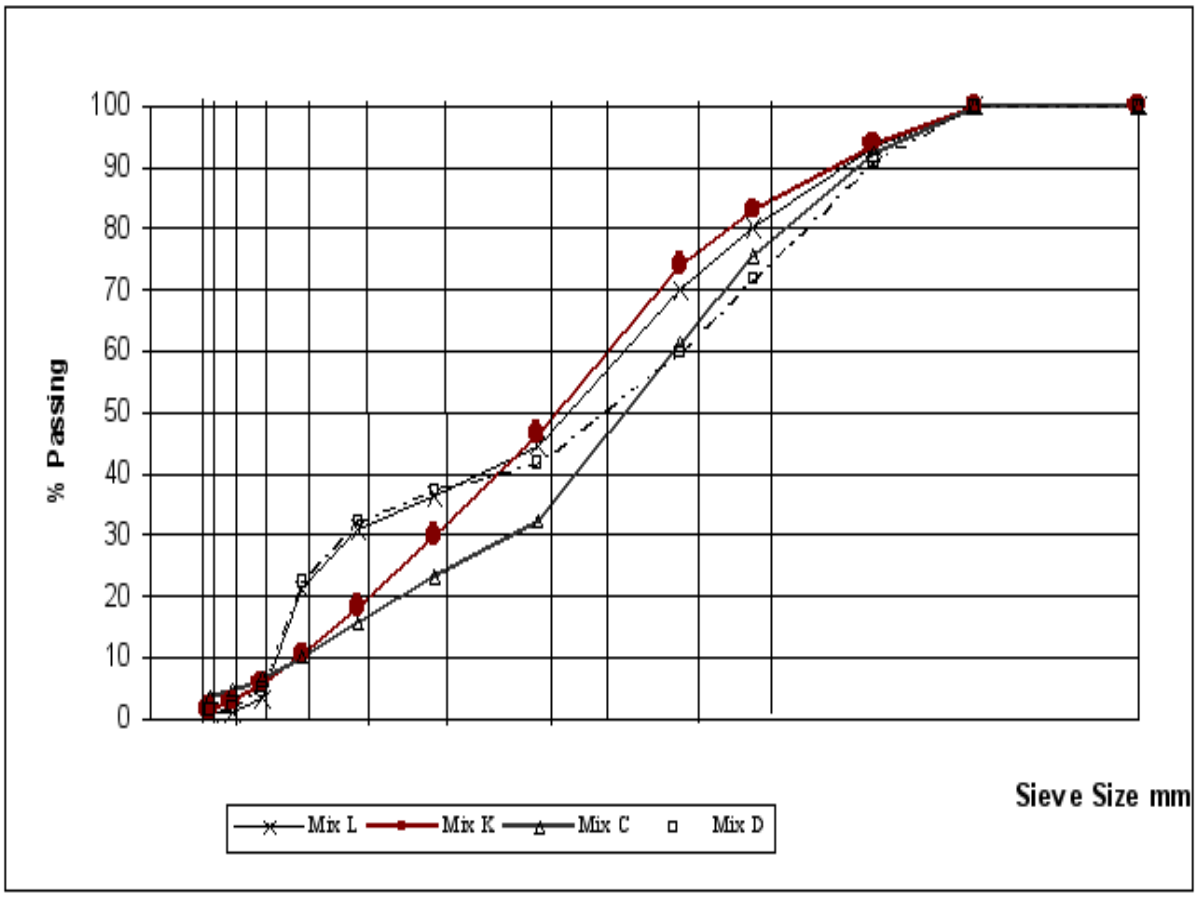

Fig. 2. Gradation Curves for the 4 Mixes.

where, G_{mm} = rice specific gravity of the asphalt mix, A = mass of oven dry sample in air and C = mass of water displaced by the sample. The compacted specimens will have air voids in it, and hence the bulk specific gravity of the specimen with the air voids will be less than the rice specific gravity of the mix. The bulk specific gravity of the sample is the ration of the weight of a unit volume of a compacted specimen (including permeable air voids) at 250 C to the weight of an equal volume of gas-free distilled water at the same temperature. The detailed procedure for carrying out this test is described in AASHTO T166. The compacted specimen is dryed in air for 2-3 days. The dry weight of the specimen in air is measured (A). The specimen is immersed in a water bath at 250 C for 4 minutes and the weight of the specimen in water is determined (C). The specimen is taken out of water, and blotted quickly with a damp towel so as to surface dry the specimen. Then determine the weight of this surface dried specimen by weighing in air (B). Then the bulk specific gravity (G_{mb}) of the sample is given by:

$$G_{mb} = \frac{\text{A}}{\text{B - C}}$$

The percent of air voids in the specimen can be determined from Gmb and Gmm:

$$\text{Percent air voids} = \left(1 - \frac{\mathbf{G_{mb}}}{\mathbf{G_{mm}}}\right)100$$

Once the actual air voids in the sample is determined, it is compared with the target air voids. Even though the specimen is compacted for the target air voids, the actual air voids in the specimen can be different from this target air voids. If there is too much deviation between the actual air voids and target air voids, the sample is thrown and a new sample is made. After measuring the air voids, the sample is again air dried for 7 days before conducting any experiments using it. An aggregate

Table III. Mix Volumetrics

MIX	G_{mm}
C	2.538
D	2.517
K	2.490
L	2.444

gradation was obtained which will meet the specification requirements for aggregates to be used for making the samples. This is shown in table II. The gradation curves are shown in figure 2 and the mix volumetrics for the mixes used is shown in table III.

3. Preparation of Batch Mixes

After the mix design the amount of aggregates required to make one sample is determined. This is obtained by making a trial sample or from past experience. A sligthly higher quantity of aggregates is used to take care of the losses which may occur when transferring and mixing. Once the quantity of aggregates required to make a sample is determined, the required quantity of the different fractions are obtained from the mix design. Then each fraction of aggregate is carefully weighed and mixed together to obtain the batch mix.

4. Preheat Batch Mixes and Asphalt Binder to Mixing Temperature

The batch mix and the asphalt is heated to a mixing temperature of 1550C. The mixing temperature is the temperature at which the kinematic viscosity of asphalt is 170± 20 centistokes. (Centistoke is the viscosity of a liquid in centipoise divided

by the density of the liquid at the same temperature. One centipoise is 1/100 th of a poise (1 poise = 1 dyne sec per square centimeter). Water at 68.4 F has an absolute viscosity of one centipoise). The batch mix is kept in the oven at the mixing temperature for at least 4 hours. The asphalt is kept at the mixing temperature for 1 hour. Similarly, all the mixing tools and equipment is also preheated to the mixing temperature.

5. Mixing

Fig. 3. Mechanical Mixer for Mixing Asphalt with Aggregates.

Once the batch mix is preheated to the mixing temperature, the aggregate is transferred to the preheated mixing bowl. The required amount of asphalt as determined by the binder content in the mix design is carefully poured into the mixing bowl. Extreme care has to be taken at this stage since even a slight increase or decrease in the asphalt content will drastically change the properties of the asphalt concrete specimen. Also care should be taken so as to minimize the loss of asphalt which adheres to the walls of the bowl. The batch mix is mixed with the hot asphalt

at the mixing temperature using a mechanical mixer (see figure 3)

6. Oven Aging

Once the mixing is completed, the mix is spread out on a relatively wide pan and kept inside the oven at the compaction temperature (1350C) for 2 hours.. Care should be taken out so as not to lose the fines sticking to the sides of the mixing bowl in the process. The compaction temperature is the temperature at which the kinematic viscosity of asphalt is 280±30 centistokes. Also the mould and any other equipment used in the compaction process are also kept in the oven at this time.

Fig. 4. Mould Used for Sample Preparation.

7. Compaction

AASHTO TP4 provides a standard method for the compaction of cylindrical specimens of HMA using the Superpave Gyratory Compactor. After oven aging, the required amount of mix is filled in the mould in three stages. After each stage the mix is hand compacted by poking it with a spatula 20 times. The amount of mix

required is fixed by trial and error so as to get the required height of the final compacted specimen. Once the mould is filled, the mix is compacted using a servopac gyratory compactor. The mix is compacted till the air voids in the mix reduces to the required value. In the experiment, the target air voids was 7%. The samples made were of 4 inches diameter and 6 inches height. The mould for the preparation of 4 inch by 6 inch sample is shown in Figure 4. The superpave gyratory compactor has been designed to compact HMA samples to a density similar to that obtained in the field under traffic. It also tends to orient the aggregate particles similar to that observed in the field. Although the Superpave gyratory has some similarities to other gyratory compactors, it is a unique piece of equipent. There are three parameters that control the compaction effort on the Superpave machine. These settings are vertical pressure, angle of gyration and number of gyrations. For the Superpave procedure, the vertical pressure is set at 600 kPa and the angle of gyration is set at 1.25 degrees. The gyrations are applied at a rate of 30 revolutions per minute. A picture of the superpave gyratory compactor used to compact the mix is shown in figure 1. The final compacted specimen is shown in figure 5.

Fig. 5. A Compaction Specimen.

CHAPTER IV

A COMPRESSIBLE CONSTITUTIVE MODEL FOR COMPACTION STUDY OF ASPHALT MIXTURES

A. Continuum Preliminaries

In this section, some of the basic concepts of continuum mechanics are summarized. The basic definitions related to the kinematics and kinetics of bodies are introduced, also, the basic balance laws of physics namely the balance of mass, linear momentum, angular momentum and energy are presented briefly. We then discuss the role second law of thermodynamics plays in imposing restrictions on the response of materials.

1. Kinematics

Consider a body B in a configuration $\kappa_{R(B)}$. For convenience, we shall henceforth use κ_R to denote $\kappa_{R(B)}$. Let $\mathbf{X}$ denote a typical position of a material point in κ_R. Let $\kappa_{c(t)}$ denote the configuration occupied by the body B at time t. The motion of the body is defined as the one-to-one mapping which assigns to each point $\mathbf{X}$ in κ_R a corresponding point $\mathbf{x}$ in $\kappa_{c(t)}$:

$$\mathbf{x} = \chi_{\kappa_R}(\mathbf{X}; t) \tag{4.1}$$

Now, the displacement $\mathbf{u}(\mathbf{X}; t)$ that the particles may undergo is given as follows,

$$\mathbf{u}(\mathbf{X}; t) := \mathbf{x}(\mathbf{X}; t) - \mathbf{X} \tag{4.2}$$

The deformation gradient $\mathbf{F}_{\kappa_R}$ is defined through:

$$\mathbf{F}_{\kappa_R} = \quad \frac{\partial \chi_{\kappa_R}(\mathbf{X}; t)}{\partial \mathbf{X}}. \tag{4.3}$$

If $\det(\mathbf{F}_{\kappa_R}) \neq 0$, then we are able to decompose $\mathbf{F}_{\kappa_R}$, uniquely, using the polar decomposition theorem as follows,

$$\mathbf{F}_{\kappa_R} = \mathbf{R}_{\kappa_R}\mathbf{U}_{\kappa_R} = \mathbf{V}_{\kappa_R}\mathbf{R}_{\kappa_R} \tag{4.4}$$

where $\mathbf{R}_{\kappa_R}$ is a proper orthogonal tensor. $\mathbf{U}_{\kappa_R}$, $\mathbf{V}_{\kappa_R}$ are positive definite symmetric tensors and have the same eigenvalues but different eigenvectors tensors.

The left and right Cauchy-Green stretch tensors, $\mathbf{B}_{\kappa_R}$ and $\mathbf{C}_{\kappa_R}$ are defined through:

$$\mathbf{B}_{\kappa_R} := \mathbf{V}^2 = \mathbf{F}_{\kappa_R}\mathbf{F}^T_{\kappa_R} \tag{4.5}$$

$$\mathbf{C}_{\kappa_R} := \mathbf{U}^2 = \mathbf{F}^T_{\kappa_R}\mathbf{F}_{\kappa_R} \tag{4.6}$$

Consequently, the Green-St.Venant strain tensor ($\mathbf{E}_{\kappa_R}$) and the Almansi-Hamel strain tensor ($\mathbf{e}_{\kappa_R}$) are defined, respectively, in terms of $\mathbf{C}_{\kappa_R}$ and $\mathbf{B}_{\kappa_R}$.

$$\mathbf{E}_{\kappa_R} := \frac{\mathbf{C}_{\kappa_R} - \mathbf{I}}{2} \tag{4.7}$$

$$\mathbf{e}_{\kappa_R} := \frac{\mathbf{I} - \mathbf{B}^{-1}_{\kappa_R}}{2} \tag{4.8}$$

The velocity $\mathbf{v}$ of a material point is defined as,

$$\mathbf{v} := \frac{\partial \chi_{\kappa_R}(\mathbf{X}; t)}{\partial t} \tag{4.9}$$

The velocity gradient, $\mathbf{L}$, is related to the deformation gradient $\mathbf{F}_{\kappa_R}$ through,

$$\mathbf{L} := \text{grad}\mathbf{v} = \dot{\mathbf{F}}_{\kappa_R}\mathbf{F}^{-1}_{\kappa_R} \tag{4.10}$$

The symmetric part of the velocity gradient denoted by $\mathbf{D}$ and the skew part denoted by $\mathbf{W}$ are given by,

$$\mathbf{D} = \frac{\mathbf{L} + \mathbf{L}^T}{2} \tag{4.11}$$

$$\mathbf{W} = \frac{\mathbf{L} - \mathbf{L}^T}{2} \tag{4.12}$$

2. Kinetics

Kinetics of a part/body describe the relationship between motion, deformation and their causal agents like forces and moments. Now, the concept of 'force' is a central idea in the study of kinetics associated with a physical phenomenon. Usually, in the study of continuum mechanics we represent such forces, influencing motion or deformation of a part/body, either as traction $\mathbf{t}$ or in the form of body force $\mathbf{b}$. The tractions describe the influencing forces that act through a surface $\partial\Omega$ that distinguishes the body from its surroundings. On the other hand the body forces represent those influences that donot directly come in direct contact with the part/body, for example, Gravity is considered a body force.

Cauchy has provided a famous proof that the traction vector $\mathbf{t}(\mathbf{x}, t; \mathbf{n})$ at any spatial position $\mathbf{x}$ and time t on any surface $\partial\Omega$ with normal $\mathbf{n}$ is uniquely determined by the traction vectors at $\mathbf{x}$ and time t on any three linearly independent planes. This result can be expressed in the following form,

$$\mathbf{t}(\mathbf{x}, t; \mathbf{n}) = \mathbf{T}^T\mathbf{n} \tag{4.13}$$

The second order tensor $\mathbf{T}$ appearing in the above expression for traction is famously known the *Cauchy Stress tensor*

3. The Balance Laws

The response of a force to outside influences is governed the balances laws of physics, namely the balance of mass, linear momentum, angular momentum and the balance of energy.

The balance of mass is given in Lagrangian description by

$$\rho_{\kappa_R} = \rho_t \text{det}\mathbf{F}_{\kappa_R} \tag{4.14}$$

where ρ_{κ_R} is the density in the reference configuration and ρ_t is the density in current configuration. Henceforth we shall use ρ to represent ρ_t.

The Eulerian description for the conservation of mass is given by

$$\dot{\rho} + \rho \, \text{div}(\mathbf{v}) = 0 \tag{4.15}$$

where ρ is the density and $\mathbf{v}$ is the velocity of the material. Incompressiblity reduces the above to

$$\text{div}(\mathbf{v}) = 0 \tag{4.16}$$

The conservation of linear momentum can be expresed in the form

$$\rho \left(\frac{\partial \mathbf{v}}{\partial t} + (r\mathbf{v})\mathbf{v} \right) = \text{div}\mathbf{T} + \rho\mathbf{g} \tag{4.17}$$

where $\mathbf{g}$ is the acceleration due to gravity and $\mathbf{T}$ is the Cauchy stress tensor. In the absence of internal couples, the conservation of angular momentum reduces down to the stress tensor being symmetric. That is to say

$$\mathbf{T} = \mathbf{T}^T \tag{4.18}$$

Now, the conservation of energy stipulates that the change in the energy of a system is equal to the transfer of the energy to the system. The transfer of energy could occur in various forms, however, restricting ourselves to thermomechanical processes, involving only the mechanical and thermal forms of energy, the balance of energy, in its local form gives:

$$\rho\dot{\epsilon} + \text{divq} = \mathbf{T}.\mathbf{L} + \rho r \tag{4.19}$$

where ϵ is the internal energy, q is the heat flux vector and r is the radiant heating.

4. The Second Law of Thermodynamics

The second law of thermodynamics, in the form of the Clausius-Duhem inequality, is prevalently used in continuum mechanics . In contrast, in the present work we will introduce the second law in the form of an equality by introducing a balance law for entropy, following the approach taken by Green and Naghdi [9] and Rajagopal and Srinivasa [32,33,34]. The balance law for entropy then takes the form

$$\rho\dot{\zeta} + \mathrm{div}\left(\frac{\mathrm{q}}{\theta}\right) = \rho\left(\frac{r}{\theta}\right) + \rho\Xi; \quad \Xi > 0, \tag{4.20}$$

where ζ is the entropy, θ is the absolute temperature and Ξ is the rate of entropy production. Combining the balance of energy and the balance of entropy gives the reduced energy-dissipation equation:

$$\mathbf{T}.\mathbf{L} - \rho\dot{\psi} - \rho\zeta\dot{\theta} - \frac{\mathrm{q.grad}\theta}{\theta} = \rho\theta\Xi = \xi \geq 0 \tag{4.21}$$

where ψ is the Helmholtz potential and is given by ψ= ϵ-$\theta\zeta$ and ξ is the rate of dissipation. Here, neglecting the rate of dissipation due to heat conduction, we use the reduced energy equation in the following form to place restrictions on the constitutive equations.

$$\mathbf{T}.\mathbf{L} - \rho\dot{\psi} - \rho\zeta\dot{\theta} = \hat{\xi} \geq 0 \tag{4.22}$$

B. Framework of Multiple Natural Configurations

In continuum mechanics we generally express the stress explicitly or implicitly in terms of the history of the density and various kinematical quantities in the form for constitutive relations governing material behavior. Many such constitutive descrip-

tions have been made for what is generally known as a simple material as defined by Noll [26]. For such simple materials the stress at a point is assumed to depend only on the history of quantities measured with respect to a single reference configuration (for example, the deformation gradient $\mathbf{F}_{\kappa_R}$). This assumption proves to be too restrictive to effectively describe some very common real-world material behavior.

However, Eckart [5] had long ago made the first recognition that many materials can possess multiple stress free states (natural configurations), that he called variable relaxed states, and studied them in some detail. The realization of the implications this recognition has on the symmetry considerations of the multiple stress free states and the role the evolution of the symmetry plays in the constitutive relation for the material has since been made. It is interesting to note that the symmetry state of a simple material in any configuration is known if its symmetry state is known in an arbitrarily picked reference configuration, through Noll's rule. However, in general for materials with multiple stress free configurations, the corresponding symmetry groups cannot be related by Noll's rule. An extended and detailed discussion on the natural configurations associated with various dissipative processes, with associated symmetry changes and changes in the response of the body, has been considered by Rajagopal [31,32,33].

It is in fact now considered that the notion of "Natural Configurations" is central to the development of constitutive theories in continuum mechanics. This approach to constitutive material modeling provides a rigorous thermodynamic framework. The success of such a framework in describing the response of a varied class of materials is exemplified in recent works by Rajagopal and coworkers [12,14,22,23,31,32,33,34]. This framework of multiple natural configurations utilizes the fact that upon removal of external stimuli, the body returns to a"natural configuration" that evolves, with a response of the body from these natural configurations that is non-dissiptive(elastic

response). It is assumed that the evolution of the natural configurations is determined by the preference of the body to undergo a process that maximizes the rate of dissipation. This assumption on the dissipative behavior provides us the required thermodynamic constraint to formulate a constituve response relation.

C. Development of the Constitutive Model

As discussed earlier we know that HMAs are composite three-phase materials consisting of aggregates, asphalt binder, and air voids. Their behavior is defined by the interaction between these three phases and the complex viscoelastic behavior of the binder, which depends on temperature, loading frequency, and strain magnitude. Our primary concern with modeling compaction is to study and document the influence of various mix parameters such as mix design, aggregate gradation, aggregate shape and most importantly the air void content and their distributions, on the suitability of a particular compaction method. By suitability of the compaction method we mean its close compliance to field compaction. The work done here in this regard concerns itself with effectively developing a model to corroborate the compaction curves obtained from the experiments. This will take us a long way in future attempts at modeling compaction using a thermodynamic setting.

In this work we will model HMA as a single continuum. The stored energy function and the rate of dissipation function we choose will capture the properties of HMA in a global sense. We can then demonstrate that this one constituent model can reasonably corroborate the experimental results.

Any physical/mechanical process has to satisfy the appropriate balance laws. The necessary balance laws for the problem at hand are the conservation of mass, linear and angular momentum and energy presented earlier.

For the development of the constitutive model for describing HMA mixes we adopt the framework of "Multiple Natural Configurations" as laidout by Rajagopal[31]. Now, following the framework adopted the evolution of the natural configurations is determined using a thermodynamic criterion, namely the maximization of the rate of dissipation.

Making appropriate assumptions concerning the manner in which the body stores and dissipates energy, the constitutive relations for the stress is deduced. In this work we use a compressible one constituent model for HMA. We do not take into account air voids directly in the model. However, the model captures the change in density of the HMA mixture which is closely related to the change in the air voids of the mixture.

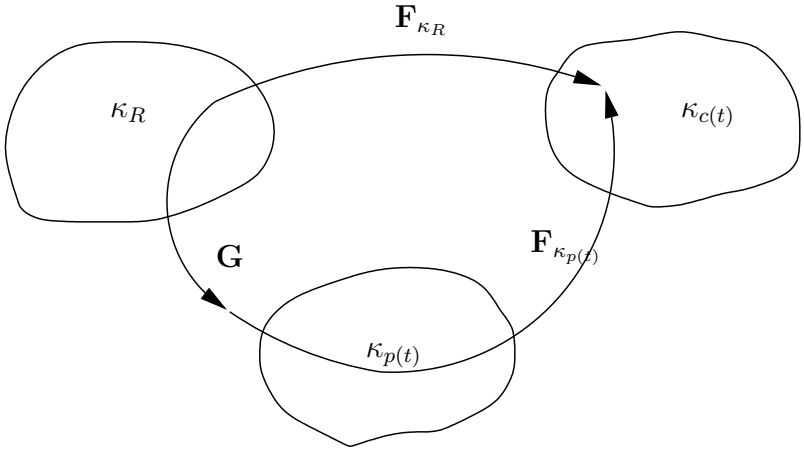

Fig. 6. Natural Configuration Associated with the Current Configuration.

Corresponding to each current configuration $\kappa_{c(t)}$ we associate a natural configuration $\kappa_{p(t)}$. In figure 6, κ_R is a reference configuration, κ_t is the configuration currently occupied by the material and $\kappa_{p(t)}$ is the natural configuration associated with the material that is currently in the configuration κ_t. The natural configuration $\kappa_{p(t)}$ corresponds to the stress free configuration associated with the current

configuration κ_t occupied by the body at time t.

In this work we shall assume just one relaxation mechanism which will effectively capture the overall relaxation of the asphalt mixture. Since we are assuming only one relaxation mechanism, we shall associate only one natural configuration, $\kappa_p(t)$ corresponding to each current configuration, $\kappa_{c(t)}$.

We assume that the asphalt mixture has an instantaneous elastic response from the natural configuration $\kappa_{p(t)}$. The gradient of the mapping from $\kappa_{p(t)}$ to κ_t is defined as $\mathbf{F}_{\kappa_{p(t)}}$. The natural configuration $\kappa_{p(t)}$ is not fixed as in the case of an elastic solid but evolves as the material is deformed. This change in the natural configuration is associated with the dissipative response of the material. We then define $\mathbf{G}$ to be the mapping between the tangent spaces of κ_R and the natural configuration $\kappa_{p(t)}$,

Therefore we have the definition,

$$\mathbf{G} := \mathbf{F}_{\kappa_R \to \kappa_{p(t)}} = \mathbf{F}^{-1}_{\kappa_{p(t)}} \mathbf{F}_{\kappa_R} \tag{4.23}$$

Now, using the conventional definition for the velocity gradient, $\mathbf{L}$ and defining the velocity gradient $\mathbf{L}_{\kappa_{p(t)}}$ associated with the natural configuration as

$$\mathbf{L}_{\kappa_{p(t)}} = \dot{\mathbf{G}}\mathbf{G}^{-1} \tag{4.24}$$

with its symmetric part given by,

$$\mathbf{D}_{\kappa_{p(t)}} = \frac{\mathbf{L}_{\kappa_{p(t)}} + \mathbf{L}^T_{\kappa_{p(t)}}}{2} \tag{4.25}$$

and we define the upper convected Oldroyd derivative of $\mathbf{B}_{\kappa_{p(t)}}$ as:

$$\overset{\nabla}{\mathbf{B}}_{\kappa_{p(t)}} := \dot{\mathbf{B}}_{\kappa_{p(t)}} - \mathbf{L}\mathbf{B}_{\kappa_{p(t)}} - \mathbf{B}_{\kappa_{p(t)}}\mathbf{L}^T = -2\mathbf{F}_{\kappa_{p(t)}}\mathbf{D}_{\kappa_{p(t)}}\mathbf{F}^T_{\kappa_{p(t)}} \tag{4.26}$$

Also similar to 4.14 we shall define the density associated with the natural configu-

ration $\kappa_{p(t)}$,

$$\rho_{\kappa_{p(t)}} = \rho \det \mathbf{F}_{\kappa_{p(t)}} = \rho \sqrt{\det \mathbf{B}_{\kappa_{p(t)}}} \tag{4.27}$$

It would also serve us later to take note that

$$\rho_{\kappa_R} = \rho_{\kappa_{p(t)}} \det \mathbf{G} \tag{4.28}$$

Now let us reconsider the reduced energy dissipation equation presented earlier in the equation 4.21

$$\mathbf{T}.\mathbf{L} - \rho\dot{\psi} - \rho\zeta\dot{\theta} - \frac{\text{q.grad}\theta}{\theta} = \rho\theta\Xi = \xi \geq 0 \tag{4.29}$$

Now, splitting the entropy production into parts due to thermal effects and that due to mechanical dissipation and considering only the mechanical part leads us to,

$$\mathbf{T}.\mathbf{L} - \rho\dot{\psi} = \hat{\xi} \geq 0 \tag{4.30}$$

In the model to be developed the effect of temperature is ignored and an isothermal model is developed. The motivation to develop an isothermal model stems from the fact that all the experimental data for compaction are obtained at a constant temperature. It is to be noted that the material parameters that will appear in the constitutive model will be different for different temperatures.

During the compaction of asphalt mixtures in a gyratory compactor, the role of asphalt mastic is in enabling the aggregate particles to move past each other. As the aggregate particles slide among each other, an optimum aggregate interlock evolves beyond which no more sliding of aggregate particles is possible. Considering that in the actual experiment the temperature reduces during compaction, the role of asphalt mastic is in aiding lubrication of aggregate particles reduces.

We assume the specific Helmholtz potential for the solid, ψ, to be defined as

follows

$$\psi = \frac{\mu(\mathbf{G})}{2\rho_{\kappa_{p(t)}}} \left(\mathrm{tr} \left(\mathbf{B}_{\kappa_{p(t)}} \right) - 3 - \ln \left(\mathrm{det} \mathbf{B}_{\kappa_{p(t)}} \right) \right) \tag{4.31}$$

And then specify the rate of dissipation due to the mechanical part ($\hat{\xi}$) in the following form,

$$\hat{\xi} = \eta(\mathbf{G}) \mathbf{D}_{\kappa_{p(t)}} . \mathbf{B}_{\kappa_{p(t)}} \mathbf{D}_{\kappa_{p(t)}} \tag{4.32}$$

Now, within the context of modeling using the framework we have chosen, we can think of the aggregate matrix and asphalt mastic as the constituents of the asphalt concrete mixture. Since, here we assume that the mixture is single constituent, the 'shear modulus' like parameter, μ, can be assumed to be a material property that characterizes aggregate matrix and the 'viscosity' function can be assumed to characterize asphalt mastic. Now, during compaction, the aggregate matrix which is initially in a loose form slowly evolves into a dense aggregate matrix (assuming, ofcourse, a homogenized form). This densification is further aided by the lubricating nature of the asphalt mastic which itself is assumed to change with deformation (in general, also with the temperature). Specific forms for the shear modulus and viscosity functions are thereby picked to represent such evolving behaviors.

Therefore, substituting the above into equation 4.31 that expresses the second law we get

$$\begin{aligned} \mathbf{T}.\mathbf{D} \quad - \quad & \rho \Bigg[2 \frac{\partial \psi}{\partial I_{\mathbf{B}_{\kappa_{p(t)}}}} \left(\mathbf{B}_{\kappa_{p(t)}} . \mathbf{D} - \mathbf{B}_{\kappa_{p(t)}} . \mathbf{D}_{\kappa_{p(t)}} \right) + 2 \frac{\partial \psi}{\partial III_{\mathbf{B}_{\kappa_{p(t)}}}} \mathrm{det} \mathbf{B}_{\kappa_{p(t)}} \left(\mathbf{I}.\mathbf{D} - \mathbf{I}.\mathbf{D}_{\kappa_{p(t)}} \right) \\ + \quad & \frac{\partial \psi}{\partial III_{\mathbf{G}}} \mathrm{det}(\mathbf{G}) \mathbf{I}.\mathbf{D}_{\kappa_{p(t)}} \Bigg] = \hat{\xi} \geq 0 \end{aligned} \tag{4.33}$$

where $I_{\mathbf{B}_{\kappa_{p(t)}}}$ and $III_{\mathbf{B}_{\kappa_{p(t)}}}$ are the first and third invariants of $\mathbf{B}_{\kappa_{p(t)}}$ and also $III_{\mathbf{G}}$ is the third invariant of the tensor $\mathbf{G}$. Rearranging the equations we get

$$\left[\mathbf{T} - 2\rho \frac{\partial \psi}{\partial I_{\mathbf{B}_{\kappa_{p(t)}}}} \mathbf{B}_{\kappa_{p(t)}} - 2\rho \mathrm{det} \mathbf{B}_{\kappa_{p(t)}} \frac{\partial \psi}{\partial III_{\mathbf{B}_{\kappa_{p(t)}}}} \mathbf{I} \right] . \mathbf{D} +$$

$$\left[2\rho\frac{\partial\psi}{\partial I_{\mathbf{B}_{\kappa_{p(t)}}}}\mathbf{B}_{\kappa_{p(t)}} + 2\rho\det\mathbf{B}_{\kappa_{p(t)}}\frac{\partial\psi}{\partial III_{\mathbf{B}_{\kappa_{p(t)}}}}\mathbf{I} - \rho\det\mathbf{G}\frac{\partial\psi}{\partial III_{\mathbf{G}}}\mathbf{I}\right].\mathbf{D}_{\kappa_{p(t)}}$$
$$= \hat{\xi} \geq 0 \tag{4.34}$$

Noticing that the R.H.S of the above equation doesnot depend on $\mathbf{D}$, and therefore equating the first term on the L.H.S to zero, we obtain the following constitutive form for stress

$$\mathbf{T} = 2\rho\frac{\partial\psi}{\partial I_{\mathbf{B}_{\kappa_{p(t)}}}}\mathbf{B}_{\kappa_{p(t)}} + 2\,\rho\det\mathbf{B}_{\kappa_{p(t)}}\frac{\partial\psi}{\partial III_{\mathbf{B}_{\kappa_{p(t)}}}}\mathbf{I} \tag{4.35}$$

thereby reducing the constraint posed by the second law to the following form

$$\left(\mathbf{T} - \rho\det\mathbf{G}\frac{\partial\psi}{\partial III_{\mathbf{G}}}\mathbf{I}\right).\mathbf{D}_{\kappa_{p(t)}} = \hat{\xi} \tag{4.36}$$

Applyin the standard method of constrained maximization with the Lagrange multiplier λ to maximize the rate of dissipation $\hat{\xi}$ with the constraint imposed by the second law (4.36), we have

$$h = \hat{\xi} + \lambda\left[\left(\mathbf{T} - \rho\det\mathbf{G}\frac{\partial\psi}{\partial III_{\mathbf{G}}}\mathbf{I}\right).\mathbf{D}_{\kappa_{p(t)}} - \hat{\xi}\right] \tag{4.37}$$

Now differentiating h with $\mathbf{D}_{\kappa_{p(t)}}$ and then equating to zero for maximization,

$$\frac{\partial\hat{\xi}}{\partial\mathbf{D}_{\kappa_{p(t)}}} + \lambda\left[\left(\mathbf{T} - \rho\det\mathbf{G}\frac{\partial\psi}{\partial III_{\mathbf{G}}}\mathbf{I}\right) - \frac{\partial\hat{\xi}}{\partial\mathbf{D}_{\kappa_{p(t)}}}\right] = 0 \tag{4.38}$$

and for our specific choice of $\hat{\xi}$, considering the dot product

$$\frac{\partial\hat{\xi}}{\partial\mathbf{D}_{\kappa_{p(t)}}}.\mathbf{D}_{\kappa_{p(t)}} = 2\,\hat{\xi} \tag{4.39}$$

leads to the equation

$$\left(\mathbf{T} - \rho\det\mathbf{G}\frac{\partial\psi}{\partial III_{\mathbf{G}}}\mathbf{I}\right) = \eta\mathbf{B}_{\kappa_{p(t)}}\mathbf{D}_{\kappa_{p(t)}} \tag{4.40}$$

Since we shall assume that the material is isotropic, we can choose (without any loss

in generality) that the configuration $\kappa_{p(t)}$ is rotated such that

$$\mathbf{F}_{\kappa_{p(t)}} = \mathbf{V}_{\kappa_{p(t)}} \tag{4.41}$$

Now premultipying equation 4.40 with $\mathbf{V}^{-1}_{\kappa_{p(t)}}$ and post multiplying it with $\mathbf{V}_{\kappa_{p(t)}}$ we obtain

$$\mathbf{T} \; - \; \rho \, \mathrm{det}\mathbf{G} \frac{\partial \psi}{\partial III_{\mathbf{G}}} \mathbf{I} = \eta \mathbf{V}_{\kappa_{p(t)}} \mathbf{D}_{\kappa_{p(t)}} \mathbf{V}_{\kappa_{p(t)}} \tag{4.42}$$

This above result along with the equations 4.26 and 4.41 results in the following

$$\overset{\nabla}{\mathbf{B}}_{\kappa_{p(t)}} = -\frac{2}{\eta} \left(\mathbf{T} \; - \; \rho \, \mathrm{det}\mathbf{G} \frac{\partial \psi}{\partial III_{\mathbf{G}}} \mathbf{I} \right) \tag{4.43}$$

In order to take into consideration the initial highly compressible behavior and the material hardening as the material reaches the limits of incompressiblity towards the end of the compaction process, we make the following choices for μ and η with arbitrary constant coefficients, $\hat{\mu}$ and $\hat{\eta}$,

$$\mu = \hat{\mu}(1 + \lambda_1 (\mathrm{det}\mathbf{G})^{q_1}) \tag{4.44}$$

$$\eta = \hat{\eta}(1 + \lambda_2 (\mathrm{det}\mathbf{G})^{q_2}) \tag{4.45}$$

Now, after performing the required differentiations of ψ and using equation 4.27 and 4.28 we obtain

$$\frac{\partial \psi}{\partial I_{\mathbf{B}_{\kappa_{p(t)}}}} = \frac{\mu}{2\rho \sqrt{\mathrm{det}\mathbf{B}_{\kappa_{p(t)}}}} \tag{4.46}$$

$$\frac{\partial \psi}{\partial III_{\mathbf{B}_{\kappa_{p(t)}}}} = -\frac{\mu}{2\rho \sqrt{\mathrm{det}\mathbf{B}_{\kappa_{p(t)}}}} \left(\frac{1}{III_{\mathbf{B}_{\kappa_{p(t)}}}} \right) \tag{4.47}$$

$$\frac{\partial \psi}{\partial III_{\mathbf{G}}} = \frac{(\mu(q_1 + 1) - q_1)}{2\rho \sqrt{\mathrm{det}\mathbf{B}_{\kappa_{p(t)}}} \mathrm{det}\mathbf{G}} \left(\mathrm{tr} \left(\mathbf{B}_{\kappa_{p(t)}} \right) - 3 - \ln \left(\mathrm{det}\mathbf{B}_{\kappa_{p(t)}} \right) \right) \tag{4.48}$$

The above derivatives along with the derived form for $\mathbf{T}$ give us the final form for the

constitutive stress as

$$\mathbf{T} = \frac{\mu}{\sqrt{\det \mathbf{B}_{\kappa_{p(t)}}}} \left(\mathbf{B}_{\kappa_{p(t)}} - \mathbf{I} \right) \tag{4.49}$$

This constitutive form is then substituted in the second law (in the form of 4.36) to obtain a constraint on $\mathbf{D}_{\kappa_{p(t)}}$. The following constaint, thereby obtained, governs which $\mathbf{D}_{\kappa_{p(t)}}$ are possible,

$$\begin{aligned} \frac{\mu}{\sqrt{\det \mathbf{B}_{\kappa_{p(t)}}}} \frac{(\mathbf{B}_{\kappa_{p(t)}}.\mathbf{D}_{\kappa_{p(t)}} - 1)}{\mathrm{tr}\mathbf{D}_{\kappa_{p(t)}}} &- \frac{(\mu(q_1+1) - q_1)}{2\sqrt{\det \mathbf{B}_{\kappa_{p(t)}}}} \left(\mathrm{tr}(\mathbf{B}_{\kappa_{p(t)}}) - 3 - \ln(\det \mathbf{B}_{\kappa_{p(t)}}) \right) \\ &= \eta \ \frac{\mathbf{D}_{\kappa_{p(t)}}.\mathbf{B}_{\kappa_{p(t)}}\mathbf{D}_{\kappa_{p(t)}}}{\mathrm{tr}\mathbf{D}_{\kappa_{p(t)}}} \end{aligned} \tag{4.50}$$

Finally substituting 4.45 and 4.46 in 4.42 gives the form for the evolution equation governing the motion as

$$\overset{\nabla}{\mathbf{B}}_{\kappa_{p(t)}} = -\frac{2}{\eta\sqrt{\det \mathbf{B}_{\kappa_{p(t)}}}} \left(\mu \mathbf{B}_{\kappa_{p(t)}} - \mathrm{k}_1 \mathbf{I} \right) \tag{4.51}$$

where we recall that μ and η are assumed to be dependant on $\mathbf{G}$ in the forms given by 4.44 and 4.45 and k_1 is given by,

$$\mathrm{k}_1 = \mu + \frac{1}{2}(\mu(q_1+1) - q_1) \left(\mathrm{tr}(\mathbf{B}_{\kappa_{p(t)}}) - 3 - \ln(\det \mathbf{B}_{\kappa_{p(t)}}) \right) \tag{4.52}$$

D. Parametric Study of Quasi-Static Compaction Problem

Here, we aim to solve a quasi-static compaction with the mold containing the mix being kept vertical and a constant load being applied on it. The mold acts as a constraint on the radial and angular displacement, therefore the problem effectively reduces to a one dimensional compression problem in the direction of applied load. The setup is schematically represented in figure 7.

We, therefore, shall assume the following form for the deformation in cylindrical

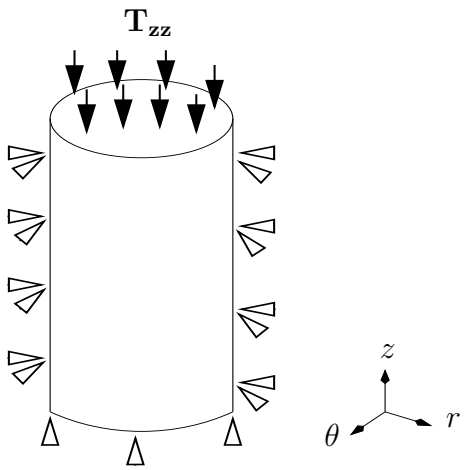

Fig. 7. Schematic for the 1-D Compression Problem.

coordinates:

$$r(t) = R(t)\ ,\ \theta(t) = \Theta(t)\ ,\ z(t) = \Lambda(t)Z(t) \tag{4.53}$$

where $\lambda(t)$ represents the stretch in the direction of loading, as a function of time. The deformation gradient referred to the reference configuration is therefore given by

$$\mathbf{F}_{\kappa_R} = \text{diag}\{1, 1, \Lambda(t)\} \tag{4.54}$$

The response from the natural configuration and the evolution of the natural configuration that are consistent with the above prescribed motion are given by

$$\mathbf{F}_{\kappa_{p(t)}} = \text{diag}\{1, 1, b(t)\}, \quad \text{and} \tag{4.55}$$

$$\mathbf{G} = \text{diag}\{1, 1, g(t)\} \tag{4.56}$$

Therefore, we have the left stretch tensor with respect to the evolving natural configurations as

$$\mathbf{B}_{\kappa_{p(t)}} = \text{diag}\{1, 1, b^2(t)\} \tag{4.57}$$

Now, from the following relationship

$$\mathbf{F}_{\kappa_R} = \mathbf{F}_{\kappa_{p(t)}}\mathbf{G} \tag{4.58}$$

we have,

$$\Lambda(t) = b(t).g(t) \tag{4.59}$$

We apply a constant compressive stress along the axial z-direction, therefore we have

$$\mathbf{T}_{zz} = \text{diag}\{0, 0, T_{zz}\} \tag{4.60}$$

The velocity gradient for the assumed deformation is given by,

$$\mathbf{L} = \text{diag}\left\{0, 0, \frac{\dot{\Lambda}(t)}{\Lambda(t)}\right\} \tag{4.61}$$

The constitutive equation for the stress in the z-direction gives us the following condition for $b(t)$

$$T_{zz} = \frac{\mu(g)}{b(t)}(b^2(t) - 1) \tag{4.62}$$

where

$$\mu(g) = \hat{\mu}(1 + \lambda_1(g(t))^{q_1}) \tag{4.63}$$

And the evolution equation in the same direction is obtained as

$$\frac{\partial B_{zz}}{\partial t} + v_z\frac{\partial B_{zz}}{\partial z} - 2L_{zz}B_{zz} = -\frac{2}{\eta(g)}\left(\frac{\mu(g)}{b(t)}B_{zz} - k_1\right) \tag{4.64}$$

where,

$$k_1 = \frac{(b^2 - 1 - 2lnb)}{2b}(\mu(g)(q_1 + 1) - q_1) + \frac{\mu(g)}{b} \tag{4.65}$$

and

$$\eta(g) = \hat{\eta}(1 + \lambda_2(g(t))^{q_2}) \tag{4.66}$$

Now using 4.57, 4.59 and 4.61 in 4.64, we obtain the following differential equation,

$$\dot{g}(t) = 2\frac{g(t)}{\eta(g)}(\mu b(t) - k_1) \tag{4.67}$$

which is to be solved in conjuction with 4.62 and the initial conditions for $b(t)$ and $g(t)$ given by

$$b(0) = 1\ ,\ g(0) = 1 \tag{4.68}$$

1. Results for the Compressive Loading along T_{zz}

The displacement as a function of the time in the z-direction is obtained by solving the differential-algebraic system of equations formed by 4.62 and 4.67 subject to the initial conditions posed by 4.68. An initial value solver (ODE15S) is employed to solve the system in MATLAB. The results obtained from such an integration are presented here as comparative plots in a parametric study of the normalized total stretch, $\Lambda(t)$. The plots presented in figures 8,9,10,11,12,13 and 14 are of normalized displacement in the direction of applied stress as a function of typical time scale of the gyratory compaction process. Also the initial 'shear modulus' and 'viscosity' can be obtained by substituting $g(t = 0) = 1$ in equations 4.63 and 4.66, for any set of parameters used.

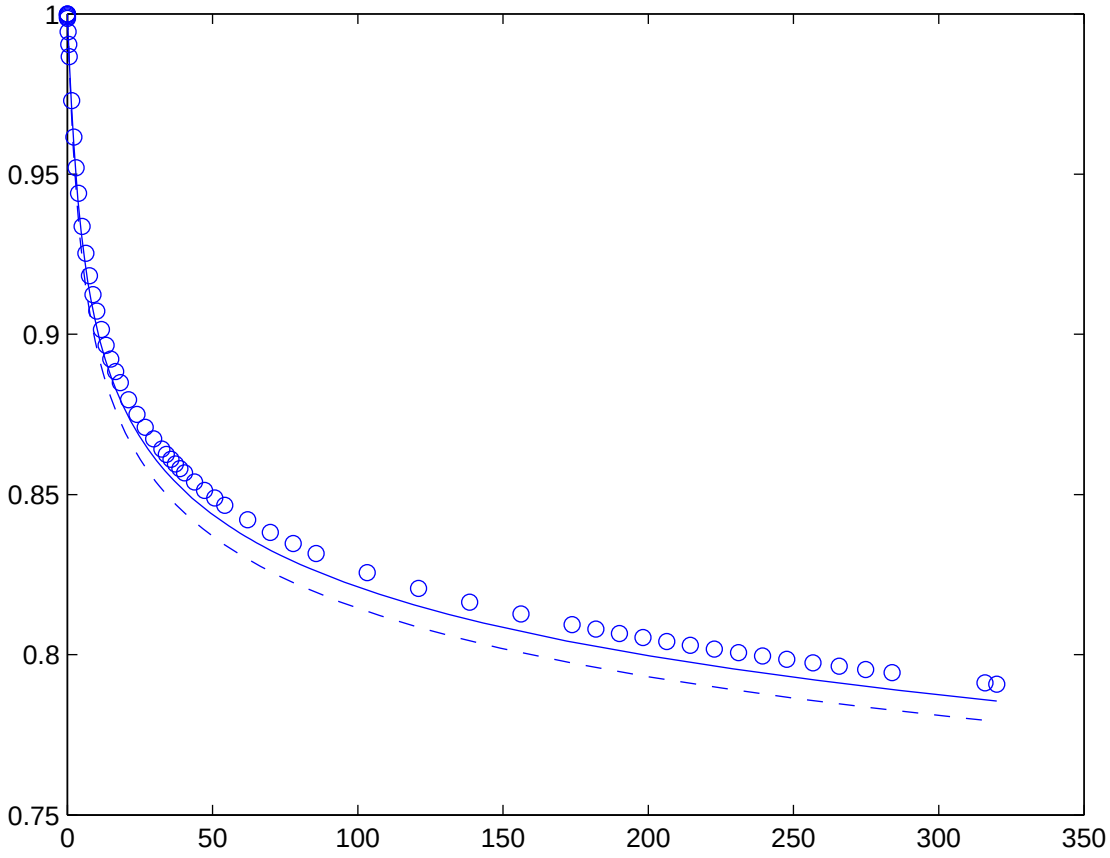

Fig. 8. Comparision for $\hat{\mu} = 20MPa, \hat{\eta} = 30MPa - s, \lambda_1 = .55, q_1 = -27, q_2 = -35$ and with Varying λ_2.

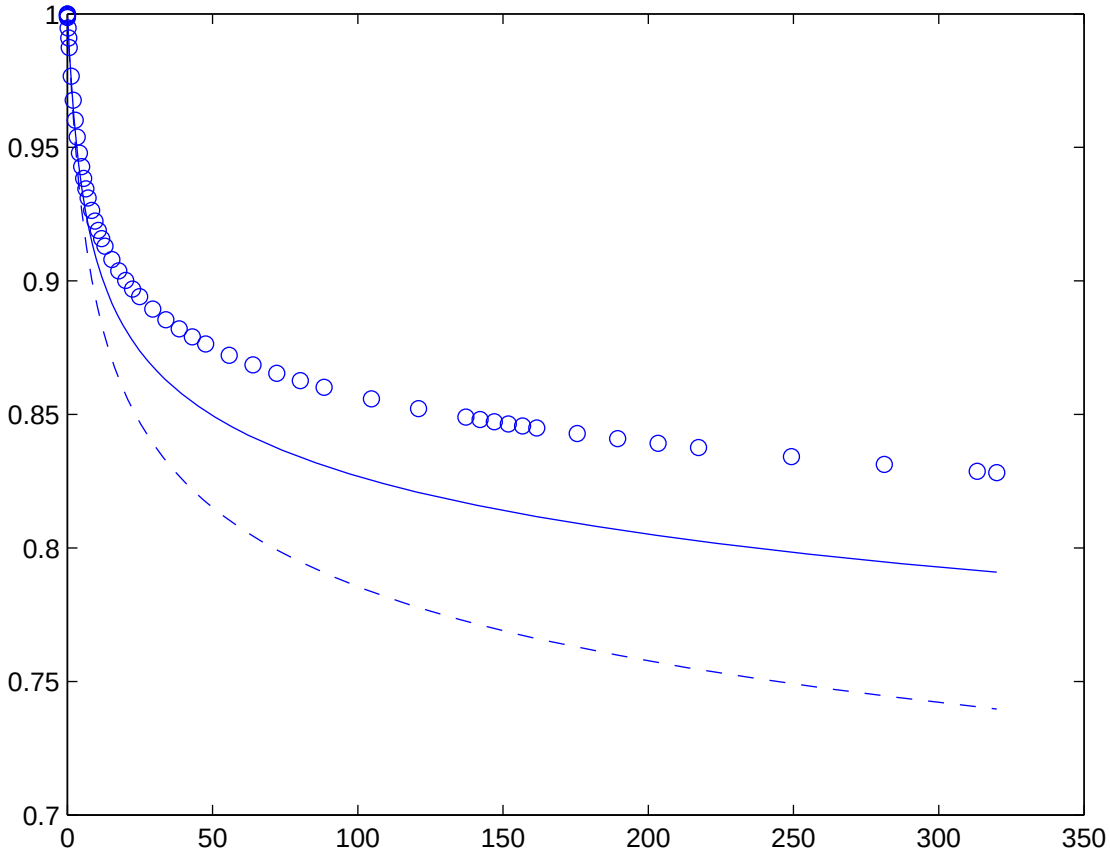

Fig. 9. Comparision for $\hat{\mu} = 20MPa, \hat{\eta} = 30MPa - s, \lambda_1 = .55, \lambda_2 = .6, q_2 = -35$ and with Varying q_1.

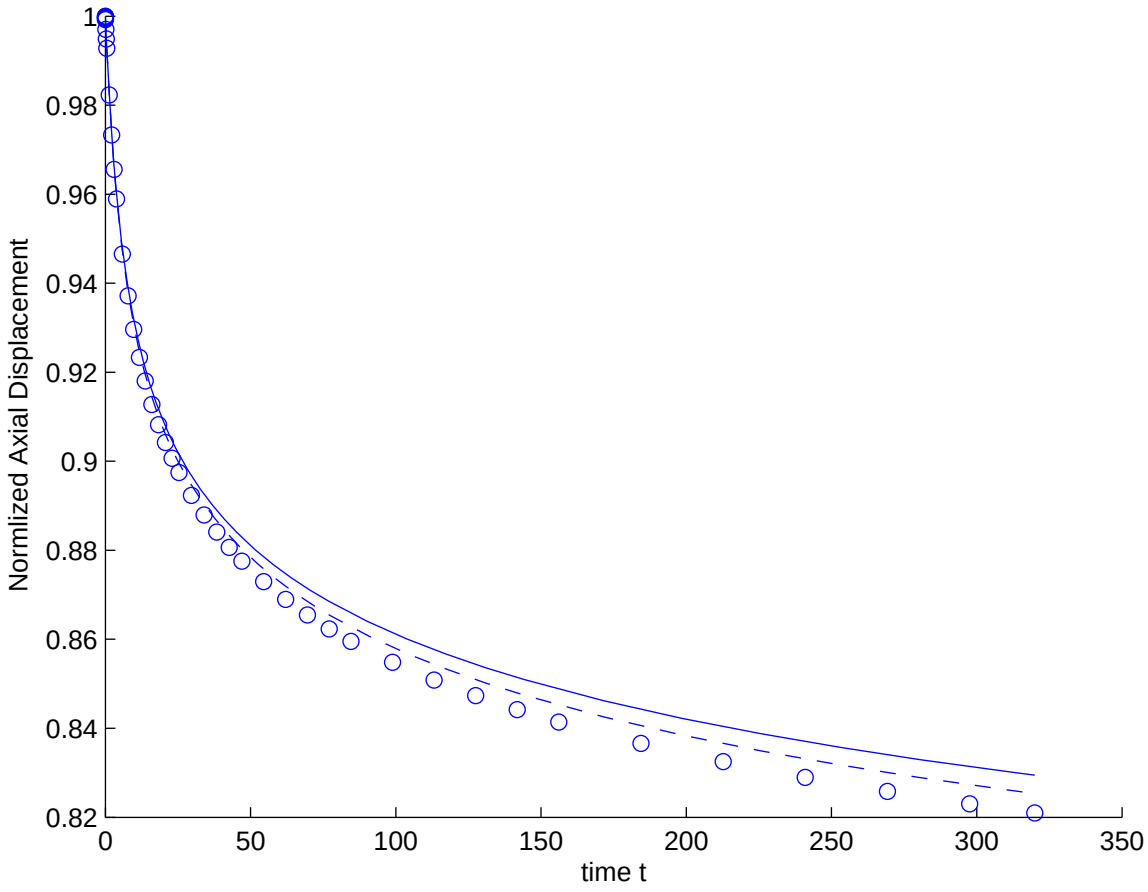

Fig. 10. Comparision for $\hat{\mu} = 40MPa, \hat{\eta} = 50MPa - s, q_1 = -25, \lambda_2 = .6, q_2 = -35$ and $\lambda_1 = 0.5, 0.6, 0.65$.

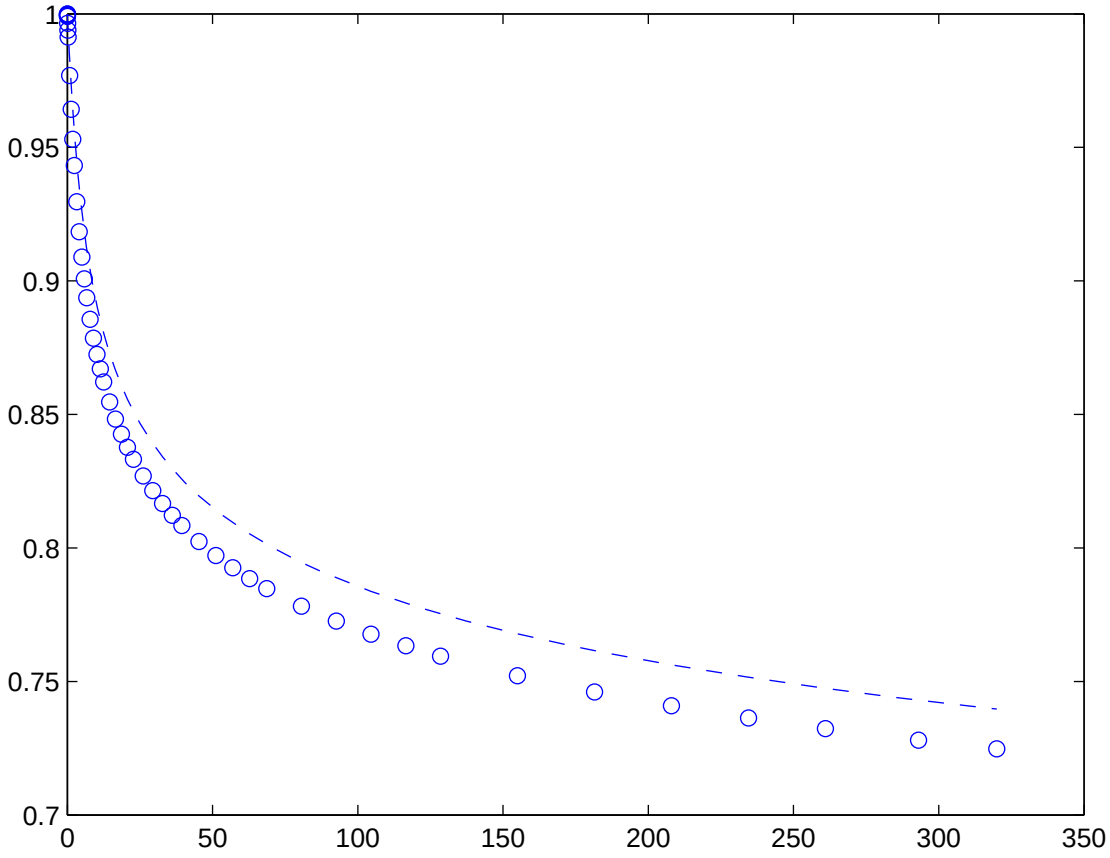

Fig. 11. Comparision for $\hat{\mu} = 20MPa, 10MPa, \hat{\eta} = 30MPa - s, 20MPa - s, \lambda_1 = .55$, $\lambda_2 = .6, q_1 = -20$ and $q_2 = -35$.

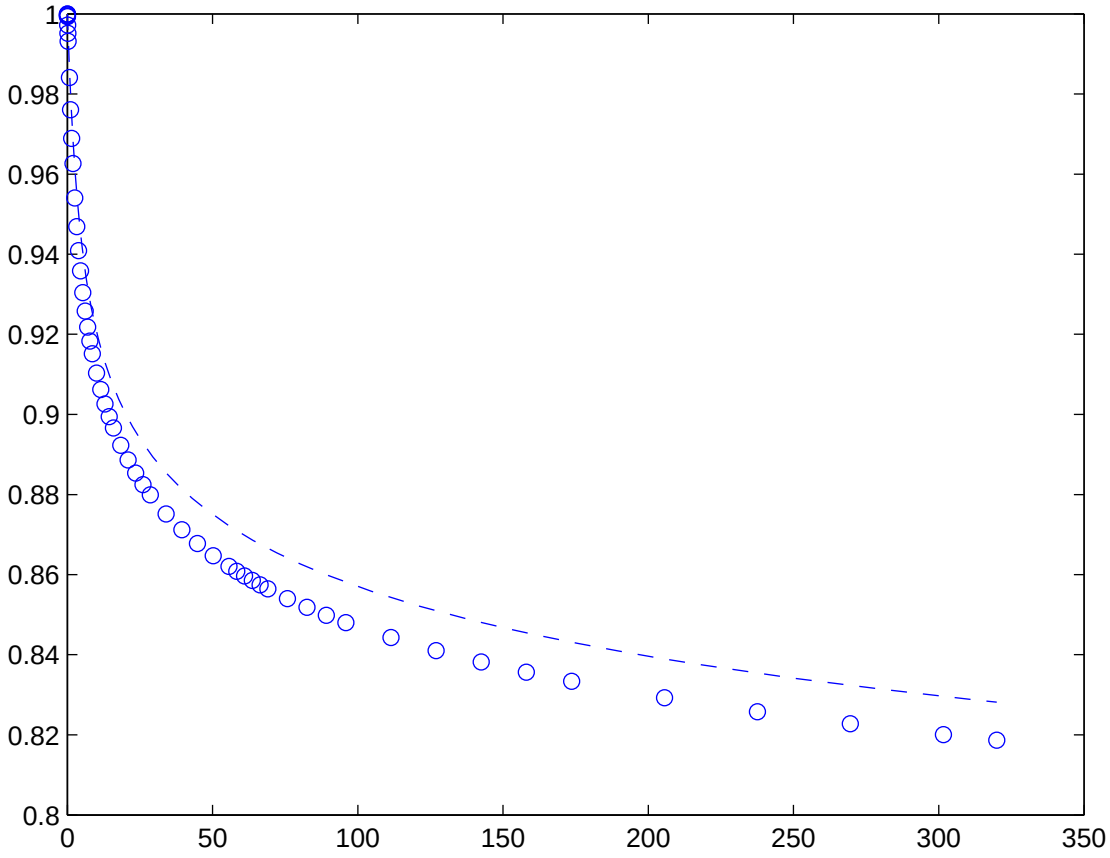

Fig. 12. Comparision for $\hat{\mu} = 20MPa, 10MPa, \hat{\eta} = 30MPa - s, 20MPa - s, \lambda_1 = .45$, $\lambda_2 = .6, q_1 = -35$ and $q_2 = -35$.

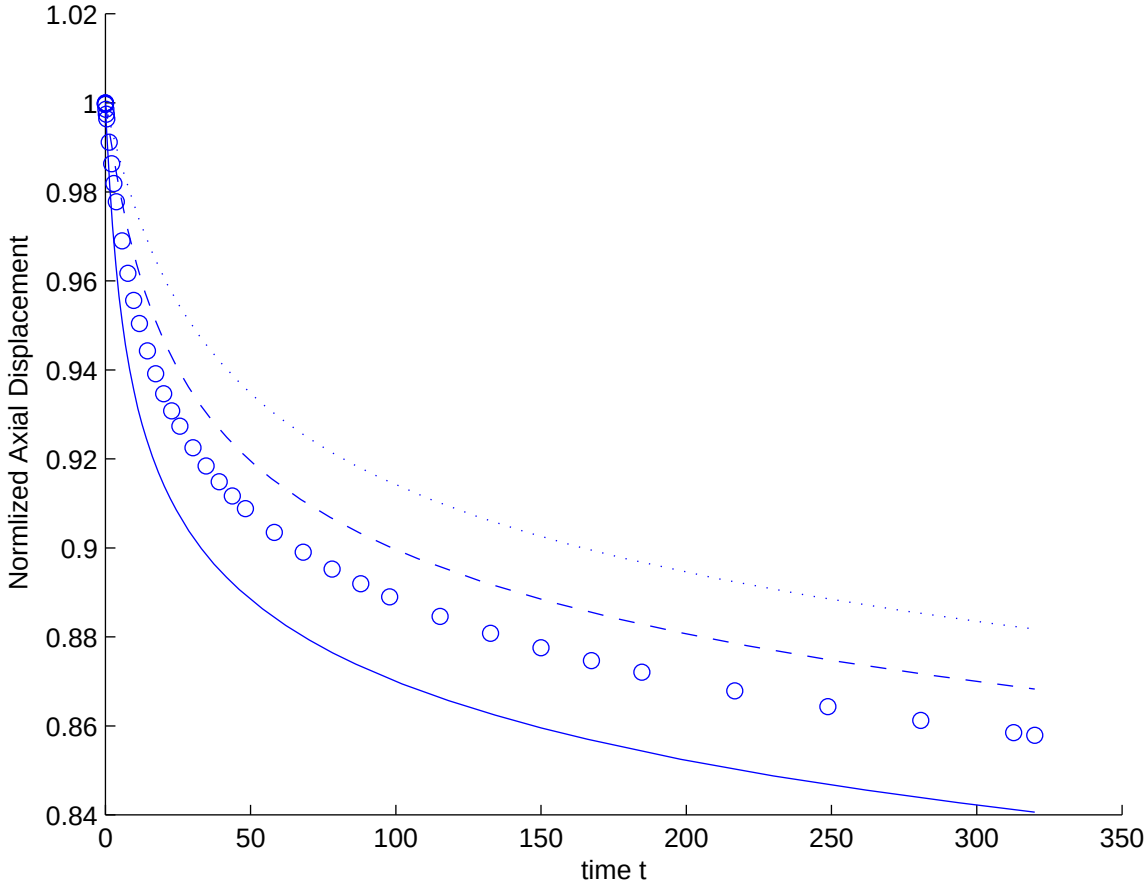

Fig. 13. Comparision for $\hat{\mu} = 40MPa, \lambda_1 = 0.5, q_1 = -25, \lambda_2 = .6, q_2 = -35$ and $\hat{\eta} = 50, 100, 150, 250MPa - s$.

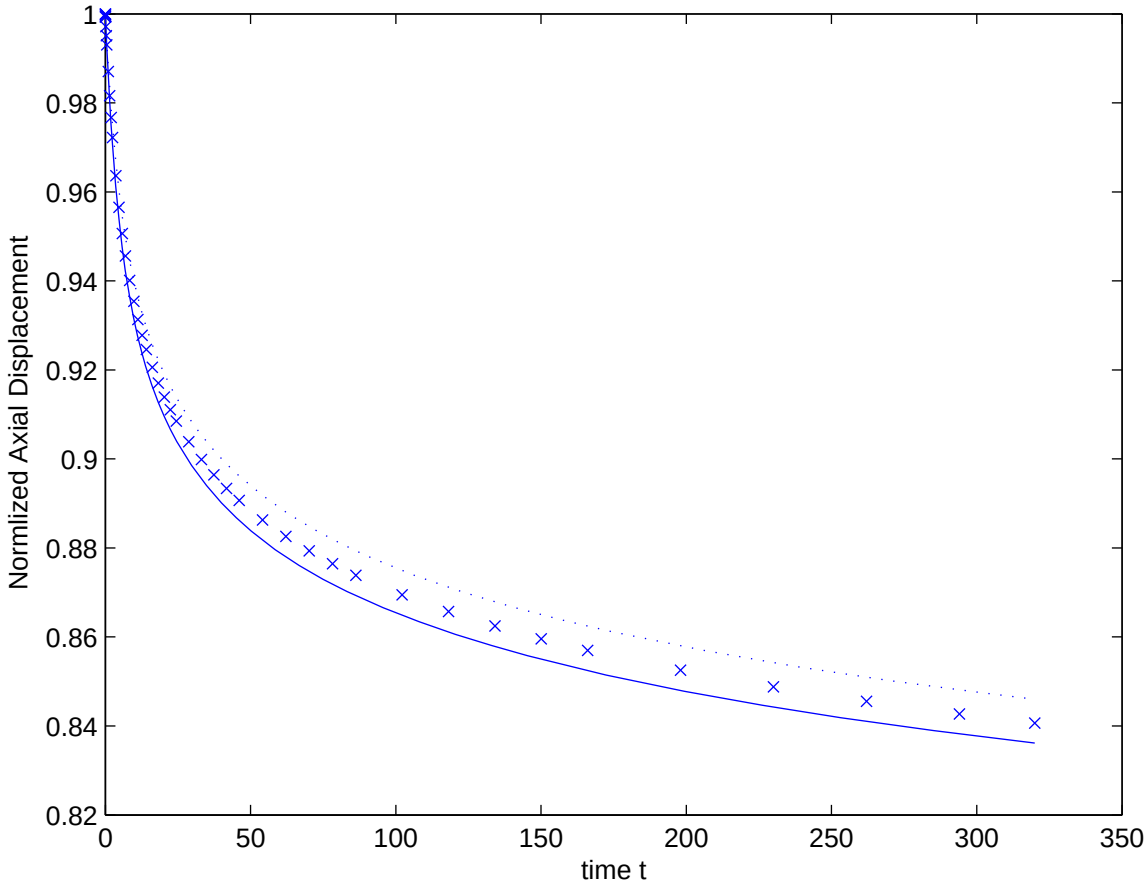

Fig. 14. Comparision for $\hat{\eta} = 50MPa - s, \lambda_1 = 0.5, q_1 = -25, \lambda_2 = .6, q_2 = -35$ and $\hat{\mu} = 40, 140, 200MPa$.

CHAPTER V

NUMERICAL IMPLEMENTATION USING FINITE ELEMENT SOFTWARE-ABAQUS

In the earlier chapter we have already briefly presented the specific problem we aim to solve. Although the final goal for the analytical modeling of the Compaction process is to be able to solve the fully dynamic problem that is a true representation of the process, we start out in this working seeking to solve the static loading case and study the time delayed effects of such a load. This approach has serves us in developing a working Finite Element model to study the complex nonlinear behavior of HMA under compaction using the theoretically framework put in place in Chapter IV.

The constitutive model developed is thereby implemented in an Finite Element program - ABAQUS/Standard. In general, for solving non-linear problems, ABAQUS provides two types of solvers, namely implicit/standard and explicit, to develop solutions numerically using the Finite Element Method. The Implicit method involves a specification of the dependent variables defined through coupled sets of equations, requiring either a matrix or iterative technique to obtain the solution. On the other hand, when direct computations for the dependent variables can be made in terms of known quantities, the solution technique is termed an Explicit method. The two solvers provided with the ABAQUS suite of software are basically developed on these premise. Our implementation of the constitutive model involves the use of user subroutine UMAT to adequately define material behavior.

A. The UMAT Facility in ABAQUS

Generally speaking, UMAT or 'user material' is a user subroutine written in Fixed-Form Fortran programming language and is used for incorporating the user defined

material models into solutions involving the ABAQUS/Standard solver. This facility makes it possible for us to define any constitutive model of varied degrees of complexity into ABAQUS and such user defined material models can be used with any ABAQUS element type. The general structure of UMAT also allows us to incorporate multiple user materials at the same time. Table IV shows a schematic representation of the interaction between ABAQUS/Standard and UMAT for large deformation analyses based on continuum formulation. We present a schematic representation of the interfacing of the UMAT with a typical ABAQUS/Standard solver:

Table IV. Schematic for the UMAT- ABAQUS Interface

ABAQUS/Standard Solver	
i) Solves the equilibrium equation in a quasi-static manner (at each time increment) ii) Carries out large deformation analysis	
$\Downarrow$	$\Uparrow$
Provides $\mathbf{F}_{\kappa_R}(t)$, $\mathbf{F}_{\kappa_R}(t+\Delta t)$, $\mathbf{F}_{\kappa_{p(t)}}$, $\mathbf{T}(t)$, $\mathbf{G}(t)$	Returns $\mathbf{F}_{\kappa_{p(t)}}(t+\Delta t)$, $\mathbf{T}(t+\Delta t)$, $\mathbf{G}(t+\Delta t)$
$\Downarrow$	$\Uparrow$
User Subroutine UMAT	
a) Use fourth order Runge-Kutta method to solve implicit ODEs for the evolution of the components of $\mathbf{B}_{\kappa_{p(t)}}$ b) Uses forward difference for obtaining numerical equations for the ODEs c) Provides convergence jacobian, DDSDDE d) Updates stress, STRESS, calculated using the constitutive relationship.	

Provided with the proper geometric model with the necessary loads defined appropriately, in a large deformation analysis based on continuum formulation, ABAQUS provides the values of total deformation gradient, $\mathbf{F}_{\kappa_R}$ at the current time t, the de-

formation gradient from the current natural configuration, $\mathbf{F}_{\kappa_{p(t)}}$ at current time t, current value of the Cauchy stress, $\mathbf{T}$ and the state variables such as $\mathbf{G}$ at the current time step, for every integration point in any element. ABAQUS also sends an estimate of the total deformation gradient at the next time step $(t + \Delta t)$. The UMAT supplies the values of the state variables such as $\mathbf{F}_{\kappa_{p(t)}}$ and $\mathbf{G}$ and Cauchy stress at time step $(t+\Delta t)$ and then returns it back to the ABAQUS. These processes continue until a converged solution is obtained at time step $(t + \Delta t)$. In estimating the value of total deformation gradient at time $(t + \Delta t)$, ABAQUS uses the value of the jacobian, DDSDDE, which is required to be specified in the UMAT. An exact definition of the consistent jacobian is necessary to ensure quadratic convergence however in many cases involving complicated material definitions, the jacobian is approximated in favor of a simpler algorithm and computational speed, this may result in the loss of quadratic convergence. In the current work, we too have used only an approximate jacobian as computational expense is really not the issue here but rather the nonlinearity in the model is.

B. Numerical Scheme for Implementation of Material Model

The UMAT to be developed to define material behavior using the model presented in the earlier chapter is for an isotropic compressible rate type material. The relevant differential equations are integrated explicitly using the fourth-order Runge-Kutta method.

1. The UMAT Development

Consider the evolution equation obtained for $\mathbf{B}_{\kappa_{p(t)}}$ given by equation 4.49. Now let us denote the right hand side of 4.49 with $\mathcal{H}\left(\mathbf{B}_{\kappa_{p(t)}}\right)$ and combine 4.49 to obtain at

any time increment

$$\dot{\mathbf{B}}_{\kappa_{p(t)}}(t) - \mathbf{L}(t)\mathbf{B}_{\kappa_{p(t)}}(t) - \mathbf{B}_{\kappa_{p(t)}}(t)\mathbf{L}^T(t) = \mathcal{H}\left(\mathbf{B}_{\kappa_{p(t)}}(t)\right) \tag{5.1}$$

The above represents a set of six implicit ordinary differential equations in time for the six independent components of $\mathbf{B}_{\kappa_{p(t)}}$. Now for an incremental change Δt we obtain the following explicit relation which can be integrated by a suitable numerical method to obtain solutions at different increments in time

$$\mathbf{B}_{\kappa_{p(t)}}(t+\Delta t) - \mathbf{B}_{\kappa_{p(t)}}(t) = \Delta t\left[\mathbf{L}(t)\mathbf{B}_{\kappa_{p(t)}}(t) + \mathbf{B}_{\kappa_{p(t)}}(t)\mathbf{L}^T(t) + \mathcal{H}\left(\mathbf{B}_{\kappa_{p(t)}}(t)\right)\right] \tag{5.2}$$

The solution using the UMAT require the specification of the consistent jacobian DDSDDE given by $\frac{\partial \Delta \mathbf{T}}{\partial \Delta \mathbf{E}}$, where $\mathbf{E}$ is a strain measure with respect to the natural configuration.

Numerically,

$$\Delta \mathbf{E} = \frac{\Delta \mathbf{B}}{2} \tag{5.3}$$

We are using $\mathbf{B}$ to represent $\mathbf{B}_{\kappa_{p(t)}}(t)$. Therefore, we have the jacobian as

$$\frac{\partial \Delta \mathbf{T}}{\partial \Delta \mathbf{E}} = 2\frac{\partial \Delta \mathbf{T}}{\partial \Delta \mathbf{B}} \tag{5.4}$$

Now using the form given by 4.47 for the constitutive stress $\mathbf{T}$ we obtain the required incremental stress as follows,

$$\Delta \mathbf{T} = \frac{\mu}{\sqrt{\det \mathbf{B}}}\Delta \mathbf{B} \tag{5.5}$$

This expression provides us with a complicated form for the jacobian which is given in component form (using δ_{ij}, the Kronecker Delta function) as follows,

$$\left[\frac{\partial \Delta \mathbf{T}}{\partial \Delta \mathbf{E}}\right]_{ijkl} = 2\frac{\mu}{\sqrt{\det \mathbf{B}}}\left[\delta_{ik}\delta_{jl} - \frac{1}{2\det \mathbf{B}}\left(\frac{\partial \det \mathbf{B}}{\partial \mathbf{B}}\right)_{kl}\mathbf{B}_{ij}\right] \tag{5.6}$$

This jacobian is then programmed to get updated at the end of each increment and this controls the convergence rate of the solution variables. The stress is also updated at the end of increment befoe it is passed to the solver for an iterative convergence through the array variable STRESS. ABAQUS uses the jacobian and the stress updates to obtain an iteratively converged solution through a Newton-Raphson scheme written into the program.

2. Geometric Model for the Quasi-Static Problem

The 3-dimensional geometry representing the compaction problem is prepared using ABAQUS/CAE, boundary conditions specified are the constraints in the radial and angular directions. An cylindrical datum coordinate system is defined to aid in this purpose and the boundary conditions are prescribed with respect to this cylindrical coordinate system. The load applied is a distributed compression pressure of magnitude 600kPa, which represents the load used in gyratory compaction experiments. A representative image of the geometry, loads and boundary conditions is shown in Figure 15. And a typical image of the finite element mesh used (3D-Continuum elements were used) is provided in Figure 16.

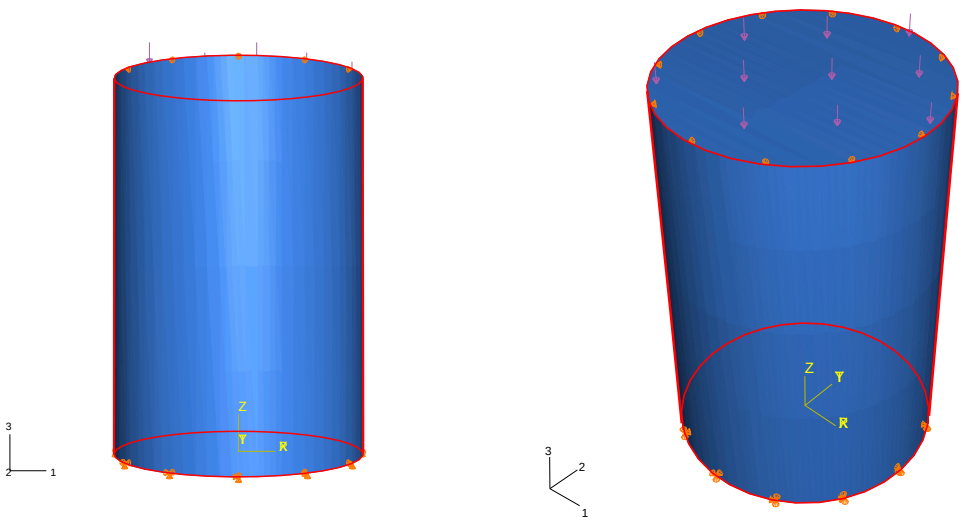

Fig. 15. Pictorial Views of the Model Geometry with Boundary Conditions.

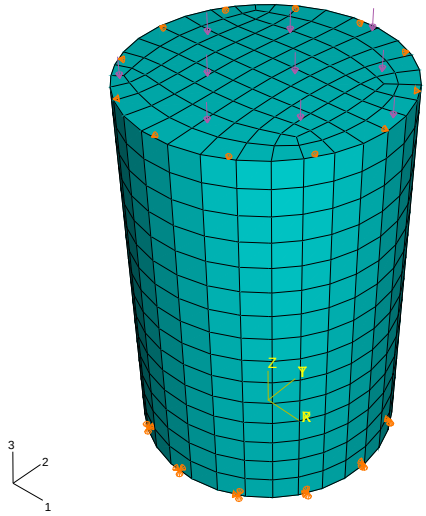

Fig. 16. Meshed View of the Model Geometry.

C. Application of UMAT to Solving the Model Developed

An input file is generated in ABAQUS/CAE, it is then linked to the UMAT and solved using the implicit solver and an iteratively converged solution for each time step is obtained. The model parameters are obtained by performing a parametric study, varying the parameters appropriately to obtain response similar to the data collected from compaction. This procedure can repeated to obtain the material parameters for different mix design and mould inclination angles. The results of the FEM analysis performed are presented in a comparative form with the results from the one dimensional solutions obtained from using MATLAB, for a few arbitrarily chosen sets of the material parameters. The aim of this exercise is to demonstrate that the theoretical model developed can be used in implementations in FEM and to show that the solutions agree with those obtained by using a different solution technique, albiet, in this case for a simple compressive deformation.

In the subsequent plots of figures 17,18 and 19, the series of circles represents Abaqus solution and the solid line, Matlab solution.

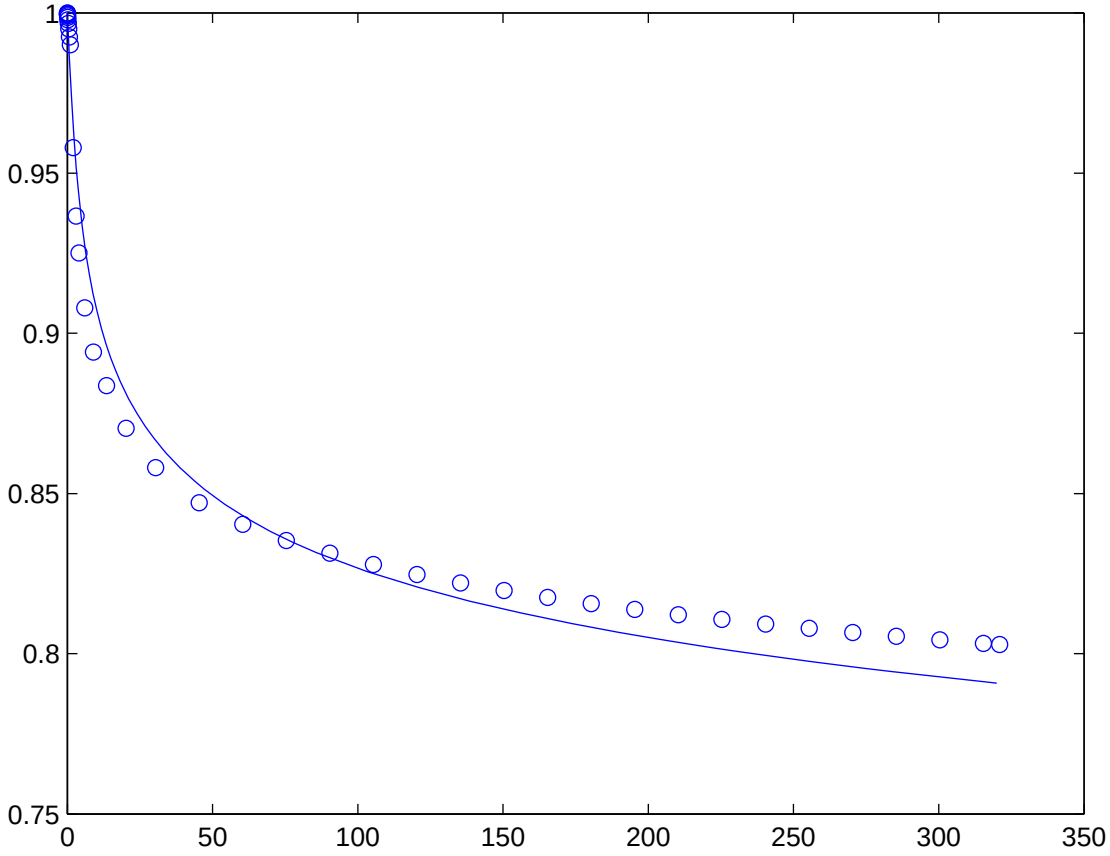

Fig. 17. Comparision of Solutions Using MATLAB and ABAQUS for $\mu = 20MPa, \eta = 30MPa - s$, $\lambda_1 = 0.55$, $\lambda_2 = 0.4$, $q_1 = -27$ and $q_2 = -35$.

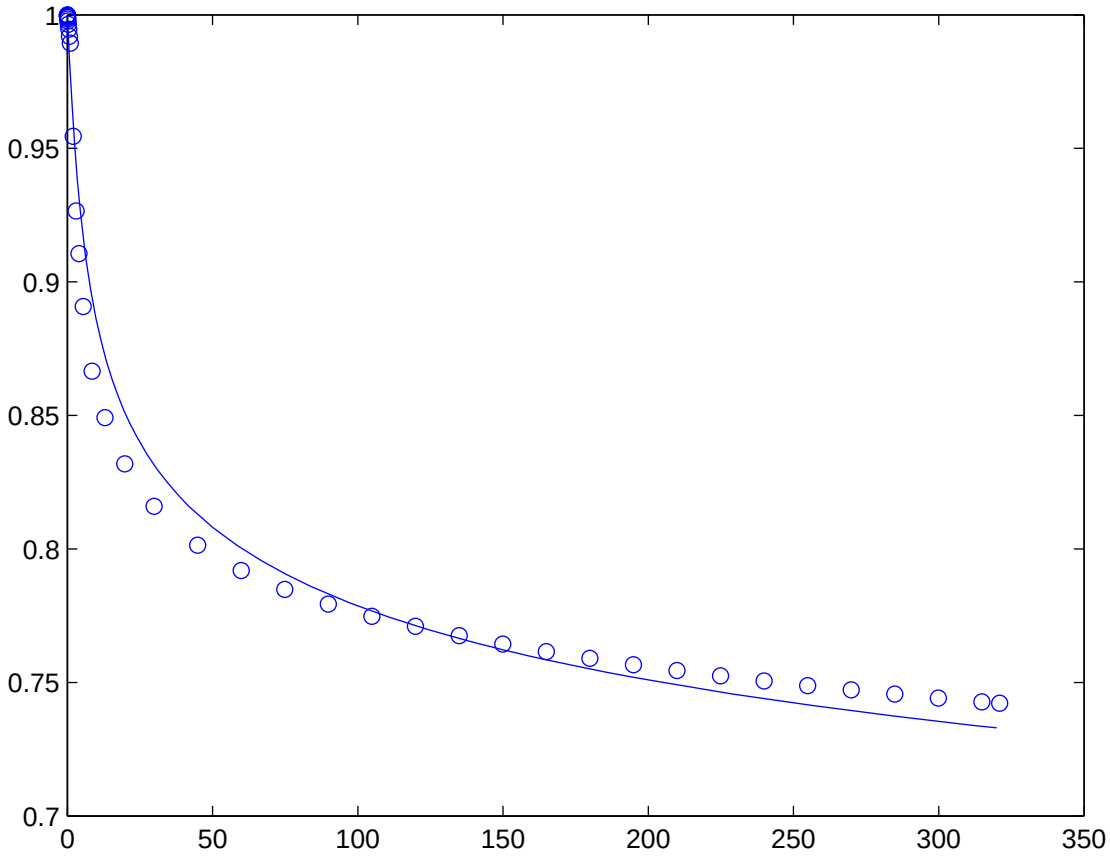

Fig. 18. Comparision of Solutions Using MATLAB and ABAQUS for $\mu = 20MPa, \eta = 30MPa - s$, $\lambda_1 = 0.45$, $\lambda_2 = 0.5$, $q_1 = -20$ and $q_2 = -25$.

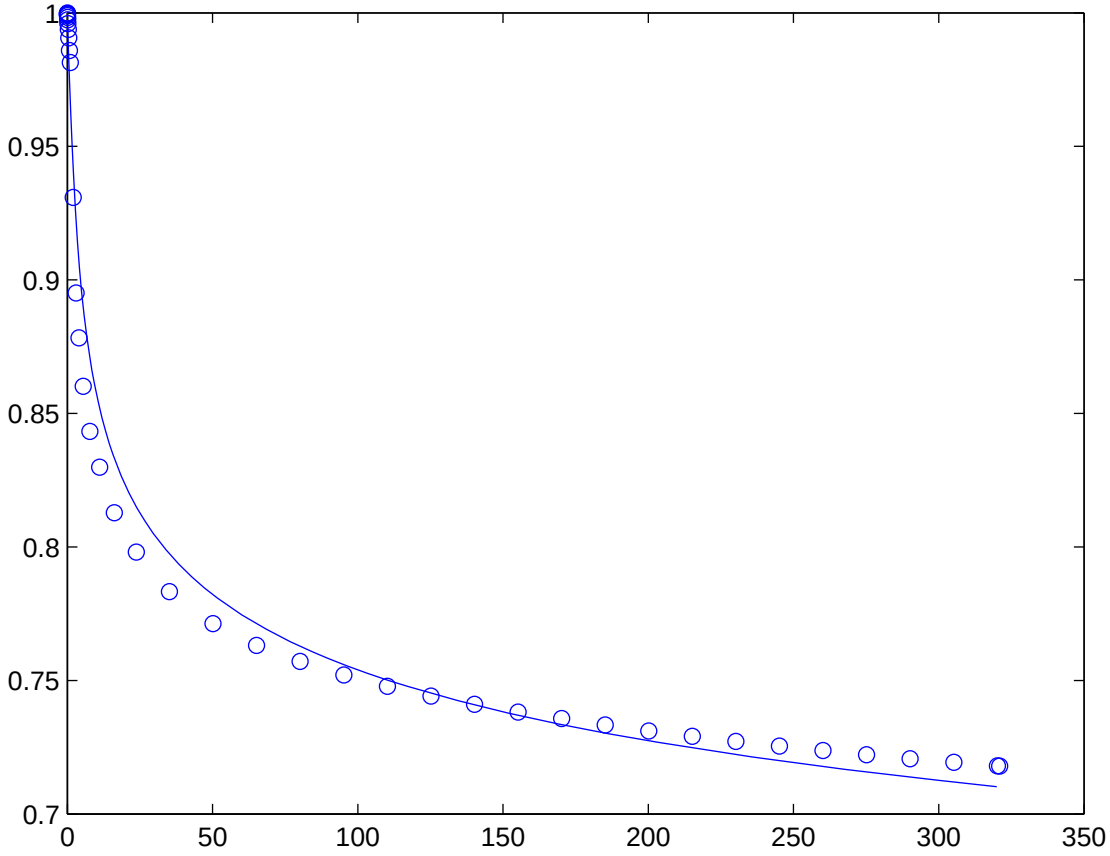

Fig. 19. Comparision of Solutions Using MATLAB and ABAQUS for $\mu = 10MPa, \eta = 20MPa - s$, $\lambda_1 = 0.65$, $\lambda_2 = 0.4$, $q_1 = -20$ and $q_2 = -25$.

CHAPTER VI

SUMMARY AND DISCUSSION OF RESULTS

A. Summary

The objective we set ourselves fro this thesis work is to be able to effectively model the compaction of asphalt composites. For this purpose we first need to establish a theoretical framework and develop the necessary constitutive relationships governing the behavior of asphalt composites under compaction. Here a framework was chosen that is based on the thermodynamics governing physical processes. A constitutive relationship has been developed that is coupled to an evolving kinematical quatity. This kinematical quantity, namely the $\mathbf{B}_{\kappa_{p(t)}}$ defined in chapter IV, governs the motion and hence the time dependant deformation of the material. The model thus developed is capable of modeling non-linear time dependant behavior of materials. It is, however, prudent to remember that the model developed represents certain idealizations in that it represents a homogenous material subject to isothermal conditions.

A simple compressive deformation seemingly representative of compaction proces (which truly is a dynamic process) is used as an example to be solved to illustrate the use of the nonlinear constitutive model developed for representing the material behavior. Here a parametric study was performed to obtain representative displacement curves in the range of deformation associated with the gyratory compaction process. The results obtained from one dimensional problem solution are compared, for a few sets of parameters, with the solutions obtained by solving the full three dimensional problem using a nonlinear Finite Element(FE) solution technique in a commercial FE solver.

B. Discussion

The parametric study performed provides us with an understanding of how each of the parameters used to define the material properties exerts influence on the evolution of the material properties, the 'shear modulus' and the 'viscosity'.It has been observed that the parameters $\hat{\mu}$ and $\hat{\eta}$ serve as the coefficents to the material functions and they govern the overall stiffness of the mix.

The values of $10MPa$ and $20MPa$ and the set $20MPa - s$ and $30MPa - a$ serve as approximate ranges for the coefficients of the two material functions for the magnitudes of deformation of interest (based on the compaction curves obtained for gyratory inclinations of 1.5, 2.25 and 3 degrees, shown in Appendix A).

The parameters q_1 and q_2 serve to govern the rate of the increase in the material parameters. With the other terms remaining unchanged we observe from the parametric study performed that higher the negative values of q_1 or q_2 quicker is the consolidation or more viscous the material behavior respectively.

λ_2 has a similar effect of accelerating the consolidation towards a solid-like behaviour and λ_1 has the effect of gradually decreasing the rate of change of magnitude of displacement with other parameters fixed. Effectively, these parameters govern the nonlinear rate of increase of the material properties.

The 'viscosity' like material property,η, determines the initial fluid like behaviour, associated with the initially dominant lubricating action of the asphalt mastic on the aggregate matrix. Increasing its initial value makes the material more and more viscous which is evident in the plot shown with changing $\hat{\mu}$. The 'shear modulus' like property,μ, determines the consolidation strength for the mix, associated with the aggregate interlock occurring due to rearrangement of the microstructure of the mix, as the mix becomes more and more dense.

The results obtained form solving the one dimensional problem compare closely with the three dimensional problem's solution. The slight deviation in results can attributed to the coarse mesh used for the FE solution. This comparison serves the purpose of demonstrating that the complex nonlinear constitutive models such as the one developed in this work can be employed to model complex material behavior using readily available numerical techniques.

C. Scope for Future Work

Future work in modeling compaction of asphalt concrete can be extended to non-isothermal models, which actually represents the compaction procedure more closely. In addition, aggregate shape and the mix structure could be accounted into the model by developing anisotropic constitutive relationships, this would then result in a non-linear theory that accounts for most of the actual physics that can be associated with the general behaviour of asphalt concretes.

REFERENCES

[1] A. R. Abbas, A. T. Papagiannakis and E. A. Masad, "Linear and nonlinear viscoelastic analysis of the microstructure of asphalt concretes," *J. Matl. Civil Engg.*, vol. 16, no. 2, pg. 133–139, 2004

[2] C. Boutin and J. L. Auriault, "Dynamic behavior of porous media saturated by a viscoelastic fluid: Application to bituminous concretes," *Int. J. Eng. Sci*, vol. 28, pp. 1157–1181, 1990.

[3] V. S. Deshpande and D. Cebon, "Steady-state constitutive relationship for idealized asphalt mixes," *Mechanics of Materials*,vol. 31, pp. 271–287, 1999.

[4] EAPA, *Asphalt in Figures 2003*, Breukelen, The Netherlands: European Asphalt Pavement Association, 2004.

[5] C. Eckart, "The thermodynamics of irreversible processes. IV. The theory of elasticity and anelasticity," *Physical Review*, vol. 73, pp. 373–382, 1948.

[6] FHA, "2002 status of the nations highways, bridges and transit: Conditions and performance," *Report to Congress FHWA-PL-03-003*, U.S. Department of Transportation, Federal Highway Administration, Washington, DC, 2003.

[7] D. Florea, "Associated elastic/viscoelastic model for bituminous concrete," *Int. J. Eng. Sci.*, vol. 32, pp. 79–86, 1994.

[8] D. Florea, "Nonassociated elastic/viscoelastic model for bituminous concrete," *Int. J. Eng. Sci.*, vol. 32, pp. 87–93, 1994.

[9] A. E. Green and P. M. Naghdi, "On thermodynamics and the nature of the second law," *Proceedings of the R. Soc. London, Ser. A*, vol. 357, pp. 253–270, 1977.

[10] M.E Gurtin, "Introduction to Continuum Mechanics," *Mathematics in Science and Engineering*, vol. 158, 2004

[11] J. Harvey and C. L. Monismith, "Effects of laboratory asphalt concrete specimen preparation variables on fatigue and permanent deformation test results using strategic highway research program A-003a proposed testing equipment," *Transportation Research Record* , Transportation Research Board, Washington, D.C.,vol. 1417, pp. 38–48, 1993

[12] K. Kannan and K. R. Rajagopal, "A thermomechanical framework for the transition of a viscoelastic liquid to a viscoelastic solid," *Math. Mech. Solids*,vol. 9, pp. 37–59, 2000.

[13] J. M. Krishnan and K. R. Rajagopal, "Review of the uses and modeling of bitumen from ancient to modern times," *Applied Mechanics Review*, vol. 56, pp. 149–214, 2004.

[14] J. M. Krishnan, K. R. Rajagopal, E. Masad, and D. N. Little, "Thermomechanical framework for constitutive modeling of asphalt concrete," *International Journal of Geomechanics*, vol. 6, pp. 36–45, 2006.

[15] J. M. Krishnan and K. R. Rajagopal, "Triaxial testing and stress relaxation of asphalt concrete," *Mechanics of Materials*, vol. 36, pp. 849–864, 2004.

[16] L. Wang, X. Wang, L. Mohammad and Y. Wang, "Application of mixture theory in the evaluation of mechanical properties of asphalt concrete," *J. Matl. Civil Engg.*, vol. 16, no. 2, pp. 167–174, 2004

[17] E. Masad, B. Muhunthan, N. Shashidhar, and T. Harman, "Effect of compaction procedure on the aggregate structure in asphalt concrete," *Transportation Research Record*, vol. 1681, pp. 179–185, 1999.

[18] E. Masad and J. W. Button, "Unified imaging approach for measuring aggregate angularity and texture," *Computer-aided Civil and Infrastructure Engineering*, vol. 15, pp. 272–280, 2000.

[19] E. Masad, L. Tashman, D. Little, and H. Zbib, "Viscoplastic modeling of asphalt mixes with the effects of anisotropy, damage and aggregate characteristics," *Mechanics of Materials*, vol. 37, pp. 1242–1256, 2005.

[20] E. Masad, B. Muhunthan, N. Shashidhar and T. Harman, "Internal structure characterization of asphalt concrete using image analysis," *J. Comput. Civ. Eng.*, vol. 13, no. 2, pp. 88–95, 1999.

[21] C. L. Monismith and K. E. Secor, "Viscoelastic behavior of asphalt concrete pavements," Tech. Rep., Inst of Transportation and Traffic Engineering, Univ of California, Berkeley, California, 1962.

[22] J. Murali Krishnan and K. R. Rajagopal, "Thermodynamic framework for the constitutive modeling of asphalt concrete: Theory and applications," *Journal of Materials in Civil Engineering*, vol. 16, no. 2 pp. 155–166, April 2004.

[23] J. Murali Krishnan and K. R. Rajagopal, "Triaxial testing and stress relaxation of asphalt concrete," *Mechanics of Materials*, vol. 36, pp. 849–864, 2004.

[24] J. Murali Krishnan and C. Lakshmana Rao, "Mechanics of air voids reduction of asphalt concrete using mixture theory," *International Journal of Engineering Science*, vol. 38, pp. 1331–1354, 2000.

[25] J. Murali Krishnan and C. Lakshmana Rao, "Permeability and bleeding of asphalt concrete using mixture theory," *Int. J. Engg. Sc.*, vol. 39, pg. 611–627, 2001

[26] W. Noll, "On the foundations of the mechanics of continous media," Carnegie Institute of Technology, Department of Mathematics, Report Vol. 17, 1957.

[27] R. W. Ogden, *Non-linear Elastic Deformations*, New York: Dover Publications, 1998.

[28] S. C. Prasad, *Constitutive Modeling of Creep of Single Crystal Superalloys*, Ph.D. Dissertation, Texas A&M Univ., College Station.

[29] P. Ravindran, *A Study of Sand-Asphalt Mixtures: A Constitutive Model Based on a Thermomechanical Framework and Experimental Corroboration*, Ph.D. Dissertation, Texas A&M Univ., College Station.

[30] P. Hariharakumar, *Constant Displacement Rate Experiments and Constitutive Modeling Of Asphalt Mixtures*, Ph.D. Dissertation, Texas A&M Univ., Collegestation, TX

[31] K. R. Rajagopal, "Multiple configurations in continuum mechanics," Report 6, Institute of Computational and Applied Mechanics, University of Pittsburgh, PA, 1995.

[32] K. R. Rajagopal and A. R. Srinivasa, " A thermodynamic framework for rate type fluid models," *Journal of Non-Newtonian Fluid Mechanics*, vol. 88, pp. 207–227, 2000.

[33] K. R. Rajagopal, and A. R. Srinivasa, "Mechanics of the inelastic behavior of materials. Part I: Theoretical underpinnings," *Int. J. Plasticity*, vol. 14, pp. 945–967, 1998.

[34] K. R. Rajagopal, and A. R. Srinivasa, "Mechanics of the inelastic behavior of materials. Part II: Inelastic response," *Int. J. Plasticity*, vol. 14, pp. 969–995,

1998.

[35] K. R. Rajagopal, "Flow of viscoelastic fluids between rotating disks," *Theoretical and Computational Methods in Fluid Mechanics*, vol. 3, pp. 185–206, 1992.

[36] F. L. Roberts, P. S. Kandhal, E. R. Brown, D. Lee, and T. W. Kennedy, "Hot mix asphalt materials, mixture design and construction," National Asphalt Pavement Association, Research and Education Foundation, Lanham, MD, 1996

[37] Samer Dessouky, E. Masad and F. Bayomy, "Evaluation of asphalt mix stability using compaction properties and aggregate structure analysis," *The International Journal of Pavement Engineering*, vol. 4, no.2, pp. 87–103, June 2003.

[38] Samer Dessouky, E. Masad and F. Bayomy, "Prediction of hot mix asphalt stability using the superpave gyratory compactor," *Journal of Materials in Civil Engineering*, vol. 16, pp. 578–587, 2004.

[39] Strategic Highway Research Program (SHRP), "Level one mix design: Material selection, compaction and conditioning," *SHRP-A-408*, National Research Council, Washington, D.C

[40] C. A Truesdell, *A First Course in Rational Continuum Mechanics*, 2nd edition *Pure and Applied Mathematics Series*, Boston: Academic Press, 1991.

[41] H.L. ter Huerne, *Compaction of Asphalt Road Pavements*, Ph.D. Dissertation, Enschede, The Netherlands, University of Twente.

[42] US Army Corps of Engineers, *Hot-Mix Asphalt Paving Handbook 2000,* location: US Army Corps of Engineers.

APPENDIX A

COMPACTION CURVES FOR ASPHALT CONCRETE MIXES

For the different mixes under consideration in our future investigations, we consider three compaction inclination angles each. The plots obtained from the gyrator compactor, the height versus number of gyrations, for each of the four mixes are provided henceforth in figures 20,21,22 and 23, (refer to chapter 3 for the nomenclature of mixes adopted here and for a brief description of mixes considered)

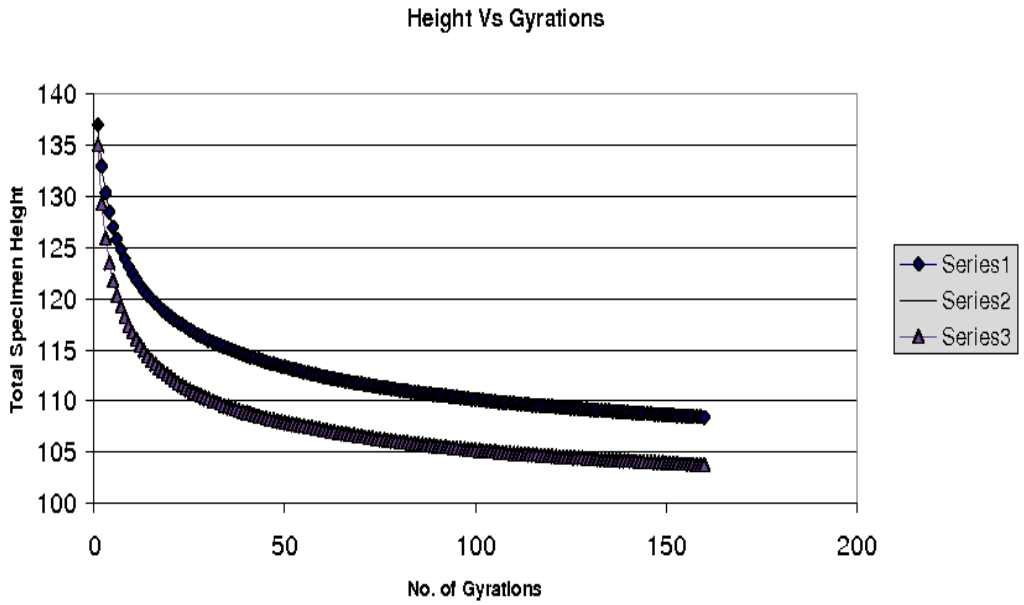

Fig. 20. Compaction Curve for the Mix C.

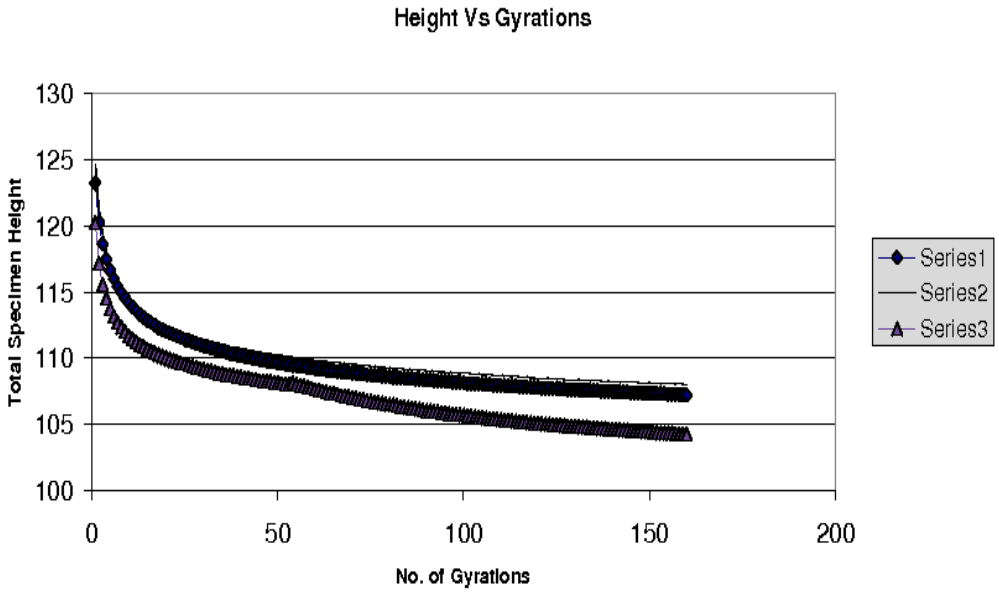

Fig. 21. Compaction Curve for the Mix D.

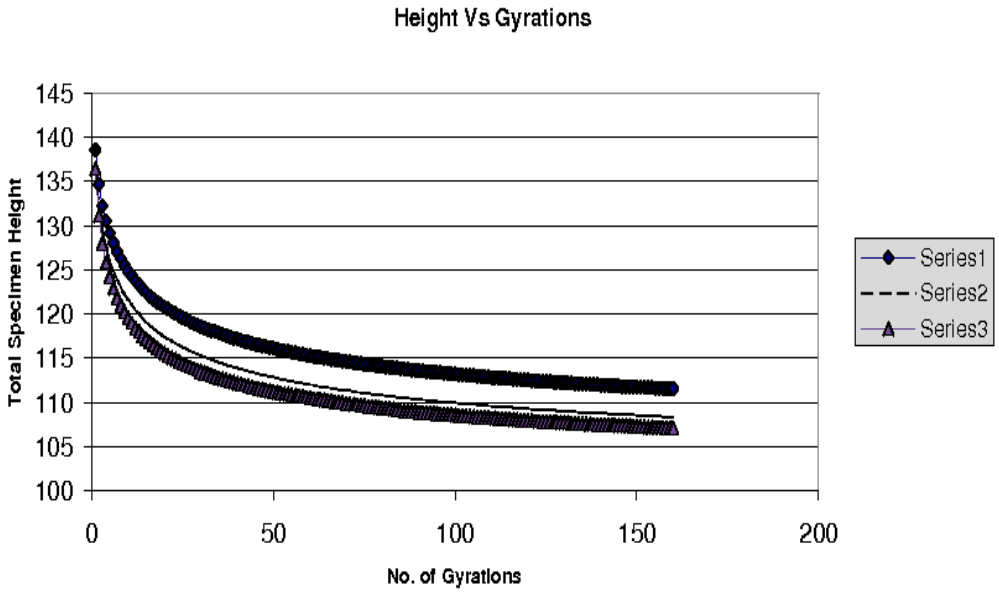

Fig. 22. Compaction Curve for the Mix K.

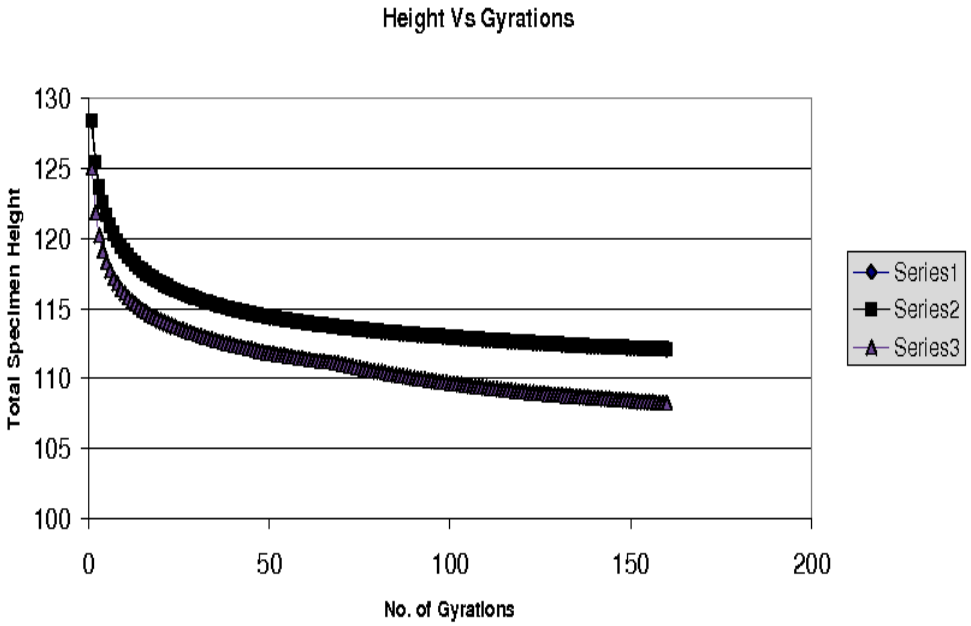

Fig. 23. Compaction Curve for the Mix L.

VITA

Saradhi Koneru was born in Hyderabad, India. He received his Bachelor of Engineering degree in mechanical engineering from the Osmania University, Hyderabad, India in June 2004 and his Master of Science in mechanical engineering from Texas A&M University in December 2006. The author may be contacted at 8-3-945/A/20, Nagarjuna Nagar, Ameerpet, Hyderabad 500073, Andhra Pradesh, India or by email at saradhi_koneru@yahoo.com.

The typist for this thesis was Saradhi Koneru.